Environmental Sciences Europe

RESEARCH

Open Access

Hydrological response of tropical rivers basins to climate change using the GR2M model: the case of the Casamance and Kayanga-Géva rivers basins

Cheikh Abdoul Aziz Sy Sadio[1], Cheikh Faye[1], Chaitanya B. Pande[2,3,4], Abebe Debele Tolche[5*], Mohd Sajid Ali[6], Marina M. S. Cabral-Pinto[7] and Mohamed Elsahabi[8]

Abstract

The main objective of this research is to evaluate the effects of climate change first on precipitation and temperature, and then on the runoff characteristics of two tropical watersheds located in Senegal and Guinea-Bissau. To achieve this, eighteen General Circulation Models (GCMs) were selected to measure various climate change scenarios under the Shared Socioeconomic Pathways (SSP) SSP1-2.6 and SSP5-8.5, using the reference period of 1985–2014. The GR2M hydrological model was employed to replicate past monthly surface runoff patterns for the Casamance and Kayanga-Géva watersheds. After calibrating and validating the GR2M model, the researchers simulated the predictable effect of climate change on the flow for the near future (2021–2040), medium future (2041–2060), and distant future (2081–2100) for each watershed, using the GCM multi-model ensemble mean. The quantile method was used to correct bias in temperature and precipitation data. The results of bias correction give a correlation coefficient greater than 0.9% for temperatures and 0,6% precipitation between the outputs of the multi-model ensemble and observations used. The results indicate also that all watersheds are expected to experience drier conditions in the near-future, mid-future, and far-future periods under both the SSP1-2.6 and SSP5-8.5 scenarios. Furthermore, the predictable temperature trends consistently show a warmer situation with growing radiative making in the future times. However, the primary factor influencing changes in flow for all watersheds is the projected precipitation changes. The anticipated drier conditions in the near-future, mid-future, and far-future horizons under both scenarios would lead to significantly reduced runoff volumes at the beginning and middle of the rainy season. Consequently, the projected seasonal changes in river flow for all catchments (e.g., under SSP5-8.5 scenario, a decline of -34.47%, -56.01%, and -68.01% was noted, respectively, for the horizons 2050, 2070, and 2090 for the Casamance basin) could lead to new frequent occurrences of drought and water scarcity associated with past hydrological regimes. These scenarios enhance the necessity of improving water management, water prizing, and water recycling policies, to ensure water supply and to reduce tensions among regions and countries.

Keywords Climate change, Modelization, GR2M, SSP, Hydrological projection, Casamance and Kayanga-Géva basins

*Correspondence:
Abebe Debele Tolche
abeberobe@gmail.com
Full list of author information is available at the end of the article

Introduction

The influence of anthropogenic climate variability on hydrological processes is well documented, affecting the energy and mass balance of these processes [42, 63, 119]. The water cycle is probable to intensify, leading to changes in hydrological patterns under dissimilar climate scenarios [119, 103, 109]. Climate change exacerbates existing challenges in water management and increases the vulnerability of water source schemes [20, 105]. To assess the possible effects of climate change on the hydrology regimes, a common approach is to use general circulation models (GCMs) and regional climate models (RCMs) to run the hydrological models through various greenhouse gas emissions scenarios [30, 75, 94]. GCMs are powerful tools for generating future climate projections [50, 84, 115]. However, they often have a low spatial resolution (100–300 km, which may not be sufficient for local impact assessment studies, especially in areas with complex terrain [54, 88, 86]. Therefore, downscaling techniques are commonly applied today, through GCM outputs with the use of higher resolution RCMs over limited areas [56, 101, 112]. However, climate models have uncertainties or biases (such as systematic, random, and parameterization biases) [23, 53, 91]. However, long-term historical data can overcome uncertainties introduced by variability in global climate models [71, 82, 117]. Large suspicions in GCM–RCM forecasts show biases in precipitation and other climate variables, making continued use of these results unpredictable for impact assessment studies [5, 113, 114, 116]. Furthermore, GCM–RCM projections often show better performance in areas with moderate climates than in tropical regions, where convective precipitation dominates and is not adequately represented by climate models [35, 48, 113, 114, 116]. Hence, applying appropriate bias correction (BC) approaches to GCM–RCM simulations becomes essential to improve the alignment of variances and observed distributions [52, 58, 111].

Climate change can modify the spatio-temporal patterns of hydrological responses in catchments [31, 78, 111]. Hydrological models have become essential tools in water resource management for tasks like flood forecasting and strategy, drought calculation, water storage and quality calculation, and studying hydrological replies in the climate change scenarios [15, 63, 99]. These models provide simplified representations of real hydrological systems to simulate believable hydrological processes using input parameters, irrespective of the climatic characteristics of the simulation historical [26, 65]. It exhibits elevations ranging from develop a framework to enhance hydrological model performances under numerous climate conditions. They argue that models are not yet (in 2018) ready to be used under different climate conditions, explaining why they develop their framework. Hydrological models can be broadly categorized into physical and conceptual approaches. Physical models utilize mathematical equations depend on mass, momentum, and energy management principles in a spatially dispersed model area [45, 60, 79]. The factor values in these models are directly related to catchment characteristics at the cell level [8, 122]. However, physical models can be challenging due to the complexity of the rainfall-flow transformation process, extensive data necessities, computational demands, over-parameterization, and factor severance [108, 22]. On the other hand, conceptual models estimated the common physical machines of hydrological developments using basic calculations, where input factors are combined into homogeneous semi-distributed or grouped objects. Conceptual hydrological models are commonly employed in water resource assessments through water balance simulations [36, 77]. These models simplify the representation of hydrological processes and often study the watershed as a system, by spatially and temporally aggregated values of input factors [21, 96]. As the parameters in conceptual models do not have direct physical interpretations, they are estimated through inverse calibration using observed historical data time series [38]. Various conceptual hydrological models, such as GR2M, have been utilized to assess water stability mechanisms in rivers [81], with surface runoff, and groundwater flow, and parameter transferability under different climate variation circumstances [2].

Hydrological model uncertainty, while in general lesser than climate model uncertainty, ought to be also accounted for in climate change impact studies, at least for near-term regional projections [34]. Hydrological simulations in natural ecosystems are always limited by simplified representation of complex processes occurring in the real world [14, 19]. However, complex physically based models do not necessarily yield better results than simpler models, especially in data-scarce regions, due to the large number of parameters and their inherent uncertainties [98]. Identifying the most suitable hydrological model for a given purpose remains an outstanding challenge for the hydrological community. Nonetheless, a multi-model approach favoring different model structures provides better characterization of different hydrological processes [14, 79].

The GR2M hydrological model [66] is extensively accepted due to its simplicity and effectiveness [11, 100]. Its semi-empirical approach has demonstrated to perform adequately when compared to similar monthly based hydrological models [43, 107]). Sensitivity analyses have determined that GR2M is sensitive to errors in precipitation data [13, 41], but comparatively robust to random errors in potential evapotranspiration data

demonstrated that the GR2M model parameters are robust to non-stationary precipitation series and that the optimized parameter values are highly correlated with land use [63, 69]. However, Guilpart et al. [37] indicate in their study of the Senegal River basin that the variability of parameters is significant. It has been widely utilized to research on the influence of climate variation on water resource accessibility [4, 11, 24, 100]. However, it is important to note that the recital of some conceptual hydrological model in varying climate situations can vary meaningfully dependent on the area, where it is applied [89]. The African continent, in particular, has been recognized as a major developing tropical "hot spot" due to anticipated decreases in total rainfall and increased inconsistency by the end of the twenty-first century as a consequence of climate change [10, 62]. Historical observations already indicate a significant increase in temperatures and a decrease in rainfall [60]. The Casamance and Kayanga-Géva watersheds are mainly susceptible to climate variation due to heavy reliance on the obtainability and circulation of water assets for critical aspects, i.e., agriculture, and drinking water supply, etc. [17, 76]. Therefore, it is essential to forecast upcoming water resources in these catchments in various scenarios to precisely assess and familiarize to the excesses of climate variation and its impacts. The objective of this research is to evaluate the upcoming variations in flow characteristics in the Casamance and Kayanga-Géva catchments by utilizing a GCM multi-model collaborative to strength a conceptual hydrological model in many climate change scenarios.

Study area

The Casamance basin is located in southern Senegal, spanning an area of approximately 20,150 km^2 between latitudes 12°20' and 13°21' north and longitudes 14°17' and 16°47' west (Fig. 1). The region experiences a Southern Sudanian climate influenced by geographical and atmospheric factors [12, 92]. The topography of the basin is characterized by low relief and gentle slopes, leading to the intrusion of the sea and subsequent salinization of farmland in some areas. The upstream area of the Casamance watershed covers 3650 km^2, situated upstream of Kolda. It exhibits elevations ranging from 80 to 10 m. The Kayanga-Geba catchment, a transboundary basin shared by Guinea, Senegal, and Guinea-Bissau, lies to the east of the Casamance watershed. Its area measures 10,325 km^2 at the Bafata station in Guinea-Bissau and 1640 km^2 at the Senegal–Guinea-Bissau border. Over the years, the Kayanga-Geba basin has experienced a notable decline in groundwater levels, resulting in severe impacts on low-water flows [76]. The Kayanga-Geba basin upstream of Wassadou encompasses 3163 km^2 and includes the Anambé sub-basin, which drains an area of 1100 km^2. The Anambé is a tributary of the Kayanga River, characterized by hydromorphic soils and seasonal flooding lasting 3 months. A dam (Niandouba Dam) situated 300 m downstream of the confluence on Senegalese territory serves as a reservoir with a storage capacity of around 50 million m^3. In summary, the Casamance basin in Senegal spans a significant area characterized by low relief and influenced by Atlantic Sudanian and Southern Sudanian climates [92]. The Kayanga-Geba catchment, shared among Guinea, Senegal, and Guinea-Bissau, has experienced declining groundwater levels, impacting low-water flows. The Anam aspects, i.e., agriculture, and drinking water supply é sub-basin, serves as a tributary to the Kayanga River and features seasonal flooding, with a dam downstream providing storage capacity.

The Kolda region which includes these two watersheds (the Kayanga watershed and the Casamance watershed) has a South Sudanian type climate [92]. This zone is located between the 900 and 1000 mm isohyets (1950–2000). The average annual temperature is 29 °C, and the hydrological regime is tropical. The assessment of the impacts of climate variability on water resources in these two basins highlights a significant rainfall deficit from the 1970s (a deficit which continued over the 1980s and 1990s) [17], followed by a slight rainfall surplus from the 2000s.

Materials

Use of GR2M and flow simulation

The GR2M hydrological model has been widely utilized for flow simulation in various studies [4, 11, 24, 43, 66, 100]. Its adoption stems from its simplicity and effectiveness, making it a valuable tool for assessing water resources. The model's semi-empirical approach has demonstrated favorable performance compared to other hydrological models with monthly time steps [4, 11, 100]. We have found that GR2M is sensitive to errors in precipitation data but relatively robust to random errors in potential evapotranspiration data [4, 24, 104]. This makes GR2M a suitable choice for simulating hydrological responses, including surface runoff and groundwater exchange, under different climate change scenarios. The model's parsimonious nature, with fewer parameters compared to physics-based models, simplifies the calibration process. Consequently, GR2M has been effectively employed to assess water balance components and evaluate the availability of water resources in various catchments. In the context of the Casamance and Kayanga-Géva watersheds, the GR2M model will be utilized to simulate the future changes in flow characteristics and provide valuable insights into the potential impacts of climate change on water resources in these regions.

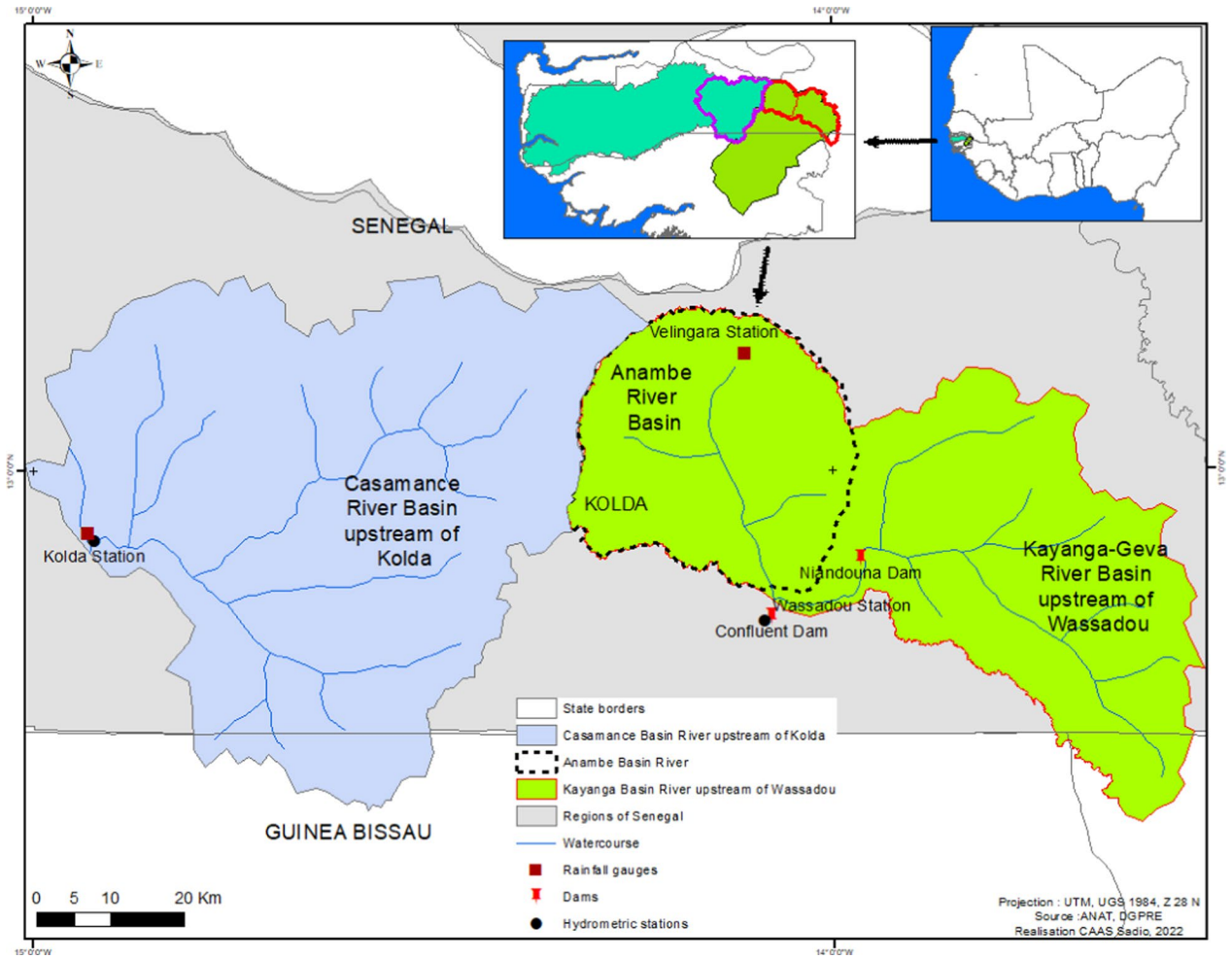

Fig. 1 Geographical location of the Casamance at the Kolda station and the Kayanga at the Wassadou station

Presentation of the GR2M model

The GR2M monthly model was chosen as the foundation for this research. The GR2M (Génie Rural à 2 parameters) model is a global rainfall–runoff model with two parameters. It was initially developed in the late 1980s at CEMAGREF (actual INRAE, Instiut National de Recherche pour l'agriculture, l'alimentation et l'environnement, in French) with the goal of applying it to water resource management. It is operating on a once-a-month period stage and has an empirical structure that resembles conceptual reservoir models. It incorporates a process for observing the moisture state in the basin, which helps account for past conditions and ensures continuous model operation. The model consists of a production reservoir, a routing reservoir, and an interface with external factors beyond the atmospheric environment [68, 66]. These components work together to simulate the hydrological behavior of basin. The GR2M model possesses qualities of robustness, simplicity, and efficiency [24, 43, 100], making it well suited for the approach proposed in this study. It has two adjustable parameters: X1, representing the maximum capacity of the production reservoir, and X2, representing the underground exchange coefficient. To use the GR2M model in a specific basin, the following data are required: the surface area of the basin in square kilometers, monthly records of rainfall (P) averaged spatially over the basin in millimeters, monthly records of potential evapotranspiration (E) in millimeters, and initial values for maximum capacity of soil storage controlled by parameter X1. The primary output of the model is the runoff at the basin outlet (Q). The structure of the GR2M model is shown in Fig. 2. P represents the monthly rainfall for month k, while E represents the average potential evapotranspiration for similar month. The model calculations govern the production, percolation, routing, and exchange processes with factors external to the atmosphere.

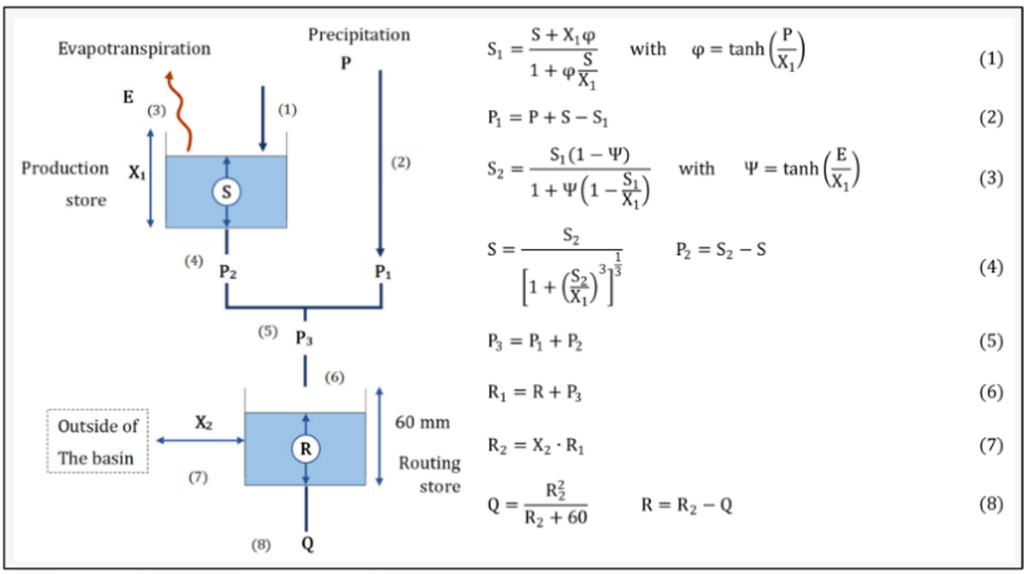

Fig. 2 Architecture of the GR2M model [65] (Source:

Data used

The monthly maximum (Tmax) and minimum (Tmin) data observed on temperature and precipitation extending from 1981 to 2021 were obtained from the National Agency for Civil Aviation and Meteorology of Senegal (ANACIM). These data are used for modeling in the Casamance basin. As for the Kayanga basin, given the missing of data in the upstream part of the basin, the maximum (Tmax) and minimum (Tmin) temperature and precipitation data from the National Aeronautics and Space Administration/Prediction of Worldwide Energy Resources (NASA/POWER) are used as alternative (from the pixels shown in Fig. 3).

Several methods make it possible, from the rainfall gauges installed in a basin, to determine the average rainfall of a basin: the weighted average of the surfaces, the method of isohyets by planimetry and the Thiessen method [24]. In the present study, the Thiessen method was used to determine the average rainfall of the basin. The choice of the Thiessen polygon method is explained by the fact that it allows weighted values to be estimated by taking into consideration each rainfall station. It assigns to each rain gauge a zone of influence whose area, expressed in%, represents the weighting factor of the local value [24]. The temperature data are used to calculate Potential Evapotranspiration using the Thornthwaite methods. This is a simple method which does not require many parameters in its calculation method and which is widely used in the literature [51, 70].

The hydrological data used in this study come from the database of the Department of Water Resources Management and Planning (DGPRE: Direction de la Gestion et de la Planification des Ressources en Eau). These are flow data from the Kolda hydrometric station, in the Casamance basin, which are only available over the period 1964 to 2008 (year from which measurements are no longer made regularly and continuously) and flow data from the Wassadou hydrometric station, in the Kayanga-Géva basin, which are only available for the period from 1976 to 2004 (year from which the measurements were stopped). The flow series used in these two basins are often incomplete and faced with a quality problem, which has impacted not only on the performance of the models on calibration and validation, but also on the periods chosen for calibration and validation.

Calibration-control and validation

The initial step in rainfall–runoff modeling involves the calibration of the model, which entails extracting the necessary information from input data (rainfall, monthly potential evapotranspiration) and output data (simulated flows) to define the model parameters that best replicate the observed flows at the catchment outlet. This calibration process ensures that the model closely mimics the hydrological behavior of the specific catchment being modeled. Typically, parameter optimization techniques are employed to approximate these behaviors.

Following the calibration phase, a model evaluation is conducted, involving testing the set of calibrated parameters on data that were not used during the calibration process (e.g., different time periods at the same station). In this evaluation stage, the set of parameters remains unchanged, and the model is used to simulate flows depend on the provided inputs. The show of the model

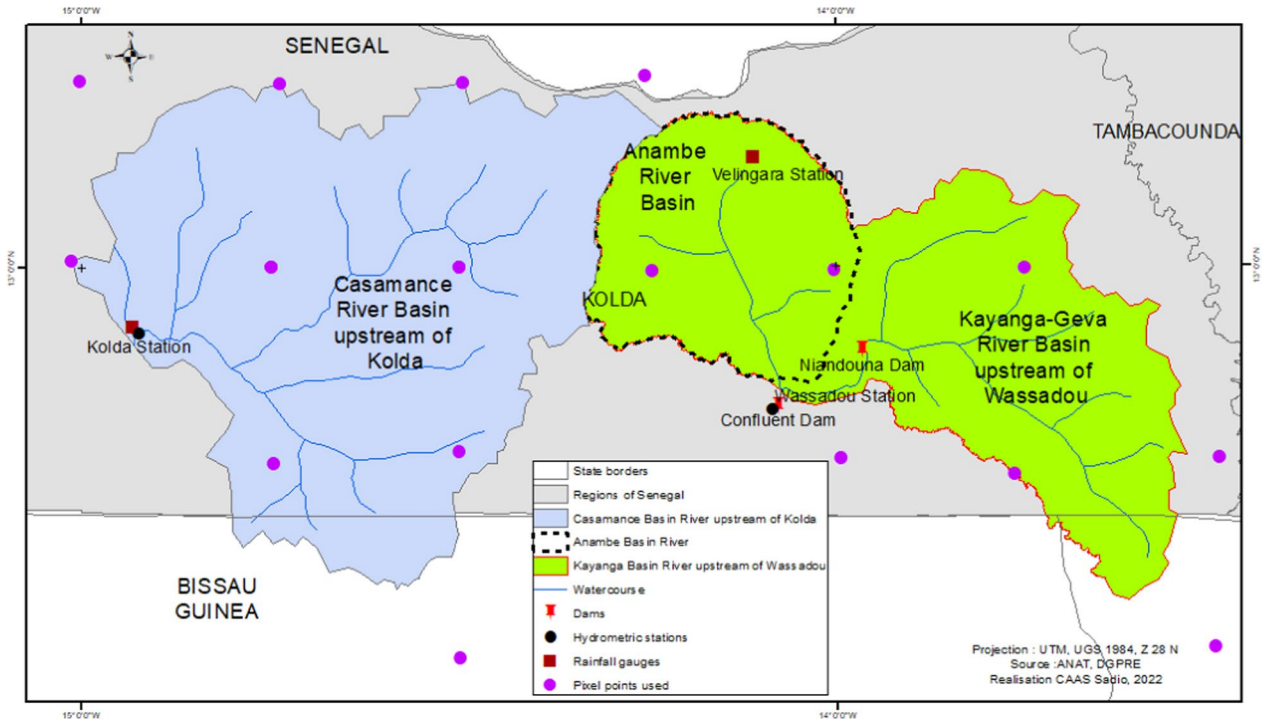

Fig. 3 Geographic location of pixels selected to determine climatic model data in the basins

can be assessed during the evaluation phase through the calculation of performance criteria. This evaluation helps identify any residual errors, assesses the model's architecture and structure, and ensures its reliability. The validation step involves applying the calibrated and evaluated model to time periods or conditions different from those used for calibration. By undertaking the calibration, evaluation, and validation stages, the rainfall–runoff model can be refined and verified to better represent the hydrological processes of the catchment.

Here, we use the GR2M conceptual model with a monthly time step which uses two parameters, and whose robustness in simulating flows in an African context has been shown in several studies [4, 11, 24, 100]. As part of this work, we seek to implement a methodology to simulate and extend hydrometric data using stations that have a minimum number of hydrometric data necessary for calibration and validation of the model.

As widely known, the calibration and verification processes are imperative for applying the mathematical model to find the most suitable model's parameters. The calibration process of the GR2M model was carried out over different periods in the Casamance and Kayanga basins, taking into account the availability and quality of flow data at the Kolda and Wassadou stations. In the Casamance basin at the Kolda station, a calibration was carried out for the period 1981–1986, followed by validation for the period 1987–1992. In the Kayanga basin, at the Wassadou station, calibration was carried out for the period 1985–1988 and validation was carried out for the period 1999–2002.

For the GR2M model, only two parameters: the production store (X1) and the groundwater exchange rate (X2), must be calibrated and validated. In this process, the appropriate initial parameters of X1 and X2 are determined. It enables the model to mimic the basin's existing hydrological behavior at the considered runoff stations before conducting the model's calibration and verification. The R-value, the initial or existing water capacity in the river, is varied between 10 and 60 mm to determine the suitable warm-up period. In our study, we found the warm-up periods of approximately 12 months (the first year of each series).

Calibrating and verifying the GR2M Model

The algorithm used to calibrate the GR2M model is the solver which is a function present in Microsoft Excel. It is a tool which allows the optimization of the parameters X1 and X2, is often used to solve equations whose operating principle is based on the calculation of the difference between the observed flow and the simulated flow. The value of the sum of the squares of the deviations is reduced by the solver to obtain the right

combination of calibration X1, X2 allowing a better fit of the model [7].

The Mann–Kendall test was used to detect possible gradual changes in the data series over the future period. According to [47] , this non-parametric test, based on rank, makes it possible to determine whether the correlation between time and the study variable is significant or not. Let (×1,....,xn) be a sample of independent values relating to a random variable X whose stationarity we seek to evaluate.

Assessment of model performance

The GR2M hydrological model is used to create a time series of *Qc* flows from rainfall (*P*) and potential evapotranspiration (*E*) inputs. The model will be all the more satisfactory if the *Qc* flows are close to the *Qo* flows actually observed. Assessing the validity of the model involves judging the proximity of the two-time series *Qo* and *Qc*. According to Hamphy [39], this analysis is useful not only for developing models but also for validating them and reducing uncertainties. To measure the accuracy of model, the outcomes are associated with hydrographs taken from field data.

The Nash–Sutcliffe index To express the correlation between the experiential values and the simulated values, we express the Nash criterion, written as:

$$Nash(Q) = 100 \times \left[\frac{\sum_{i=1}^{n} (Qsim - Qobs)^2}{\sum_{i=1}^{n} (Qsim - \overline{Q}obs)^2} \right], \qquad (1)$$

where Qsim is the simulated flow; Qobs is the observed flow; n is the number of time steps and the average of the observed flows in the series.

This is a concordance between hydrographs of between 1 and 100%, with a value of unity corresponding to a perfect correlation between observed and simulated values. It can be interpreted as the proportion of the observed flow variance explained by the model. If Nash (Q) = 100%, the fit is perfect, but if Nash (Q) < 0, the flow calculated by the model is an inferior estimate than the simple mean flow [18].

The square root of the Nash–Sutcliffe index These are the square roots of the flow rates. This criterion is more sensitive to average flow rates. Its formula is

$$Nash\left(\sqrt{Q}\right) = 100 \times \left[1 - \frac{\sum_{i=1}^{n} \sqrt{(Qsim - Qobs)^2}}{\sum_{i=1}^{n} \sqrt{(Qsim - \overline{Q}obs)^2}} \right]. \qquad (2)$$

The natural logarithm of the Nash–Sutcliffe index The Neperian logarithm of flows is more sensitive to low-water periods. Its formula is

$$Nash(lnQ) = 100 \times \left[1 - \frac{\sum_{i=1}^{n} ln(Qsim - Qobs)^2}{\sum_{i=1}^{n} ln(Qsim - \overline{Q}obs)^2} \right]. \qquad (3)$$

The combined use of these three criteria makes it possible to highlight several hydrological situations. Model performance can be judged according to the values taken by the Nash criterion [49, 67]: (1) Nash 90%: the model is excellent,(2) 80% < Nash < 90%: the model is very satisfactory; (3) 60% < Nash < 80%: the model is satisfactory; *(4)* Nash < 60%: the model is poor.

The volume balance criterion The volume balance criterion is used to compare the volumes simulated by the model with the measured volumes. The aim is to see whether, for an equivalent Nash criterion, a set of parameters that differs from the optimum obtained by calibration provides a better reproduction of the volumes flowing, both during times of high water in times of low water. This criterion therefore makes it possible to evaluate the reconciliation of the values of the observed and calculated hydrographs.

Assessment of uncertainties associated with simulated flow values Results are and always will be subject to a margin of uncertainty. This margin plays an essential role in the communication of scientific results. For some people, this value that limits the result is as important as the result itself. Errors are traditionally represented as changes between actual and simulated flow, as in the Nash criterion. However, this representation is no longer satisfactory for practice, as the similar absolute error may be slight for a flood peak and excessive for a low flow. It is, therefore, more appropriate to calculate the errors using the ratio of experiential to simulated flow [61, 80]. The expression for the uncertainty associated with the flow calculated by a hydrological model is given by the following equation:

$$I = \frac{Q_{observed}}{Q_{simulated}}. \qquad (4)$$

I is the uncertainty related with the simulated flow rate: *I is the uncertainty related with simulated flow rate, Qobserved is the observed flow rate and Qsimulated is the simulated flow rate.*

When measuring the performance of hydrological models, a criterion commonly used is the Nash criteria which evaluates the agreement between observed and simulated flows. This criterion is particularly useful for comparing model performance across different

catchments with varying flow magnitudes. Conversely, a criterion below 60% is typically considered unsatisfactory, indicating a poor agreement between observed and simulated flow. However, it is significant to note that the Nash criterion does not have an inherent lower limit. In evaluating the model performance, it is crucial to distinguish between the calibration and validation phases. While the calibration performance provides insights into how well the model reproduces observed flows during the calibration period, it may not necessarily reflect the model's ability to simulate the catchment's behavior in real-world conditions. The validation phase, on the other hand, offers a more reliable assessment of the model's simulation capabilities [85]. Therefore, the focus of the analysis of simulation outcomes should primarily be on the model's show during the validation phase.

Simulation of flows over the future period

After calibrating and validating the GR2M hydrological model, the study assessed the influences of changes in rainfall and temperature on water resource availability in the two catchments depend on upcoming climate variation scenarios. The simulations are used in the study were obtained from the latest CMIP6 simulations, as presented in the IPCC 6th Assessment Report [63, 94]. A total of 18 climate models (Table 1) were utilized (following two scenarios SSP1-2.6 and SSP5-8.5), and their outputs were ensemble-averaged to reduce natural variability and regular biases inherent in separate models [1]. The data are first evaluated on the territory of Senegal, the South-East zone in particular, and were corrected using the modified quantile method according to Bai et al. [6] which give good results compared to other methods. For temperatures, the quantile method applied is the one that uses the difference. For rainfall, the quantile method applied is that which uses a Delta Multiplicative Factor. The model data are used and corrected individually by quantile methods before the ensemble averages are used. In the Casamance and Kayanga basins, compared to the observed data from the Kolda station, the correlation coefficient of the outputs of the multi-model ensemble whose biases are corrected is greater than 0.95% for temperatures and 0.60% for precipitation, while it was around 0.9% for temperatures and 0.30% for precipitation between the observed data. And the uncorrected data (Fig. 4). Beyond bias correction, the unique use of the average ensemble will make it possible to circumvent the divergence of climate models for the future horizon and the single future trajectory (the average ensemble) will mask the uncertainties on the future climate. For future projections, the multi-model ensemble used in this study is therefore more reasonable than a single model [122].

Rainfall and temperature data were extracted from the aforementioned climate models (Table 1) in netCDF format, and ArcGIS was used to extract data from pixels located on the basin surfaces (Fig. 3), through which

Table 1 Some characteristics of the climate models used in the study

GCM name	Institute/country	Variant-id	Résolution Horizontale (Lat x Lon)
ACCESS-ESM1-5	Commonwealth Scientific and Industrial Research Organisation/Australia	r1i1p1f1	1.9°×1.2°
CanESM5	Canadian Centre for Climate Modeling and Analysis, Environment and Climate Change/Canada	r10i1p1f1	2.81°×2.81°
BCC-CSM2-MR	Beijing Climate Center/China	r1i1p1f1	1.13°×1.13°
UKESM1-0-LL	Met Office Hadley Centre/UK	r17i1p1f2	1.88°×1.25°
NorESM2-LM	Norwegian Meteorological Institute/Norway	r1i1p1f1	2.5°×1.9°
NESM3	Nanjing University of Information Science and Technology/ China	r1i1p1f1	1.9°×1.9°
MRI-ESM2-0	Meteorological Research Institute/Japan	r1i1p1f1	1.13°×1.13°
MPI-ESM1-2-HR	Max Planck Institute for Meteorology/ Germany	r10i1p1f1	0.9°×0.9°
MIROC6	Japan Agency for Marine-Earth Science and Technology/ Japan	r10i1p1f1	1.4°×1.4°
IPSL-CM6A-LR	Institut Pierre Simon Laplace/France	r10i1p1f1	2.50°×1.26°
INM-CM5-0	Institute for Numerical Mathematics/Russia	r10i1p1f1	2°×1.5°
INM-CM4-8	Institute for Numerical Mathematics/Russia	r1i1p1f1	2°×1.5°
HadGEM3-GC31-LL	Met Office Hadley Centre/UK	r1i1p1f3	1.86×1.25
GFDL-CM4	National Oceanic and Atmospheric Administration, Geophysical Fluid Dynamics Laboratory/USA	r1i1p1f1	2.5°×2.0°
FGOALS-g3	Chinese Academy of Sciences/China	r1i1p1f1	2°×2.3°
CNRM-ESM2-1	Centre National de Recherches Meteorologiques/France	r1i1p1f2	1.41°×1.41°
CNRM-CM6-1	Centre National de Recherches Meteorologiques/France	r10i1p1f2	1.41°×1.41°
CESM2	National Center for Atmospheric Research/USA	r11i1p1f1	1.25°×0.94°

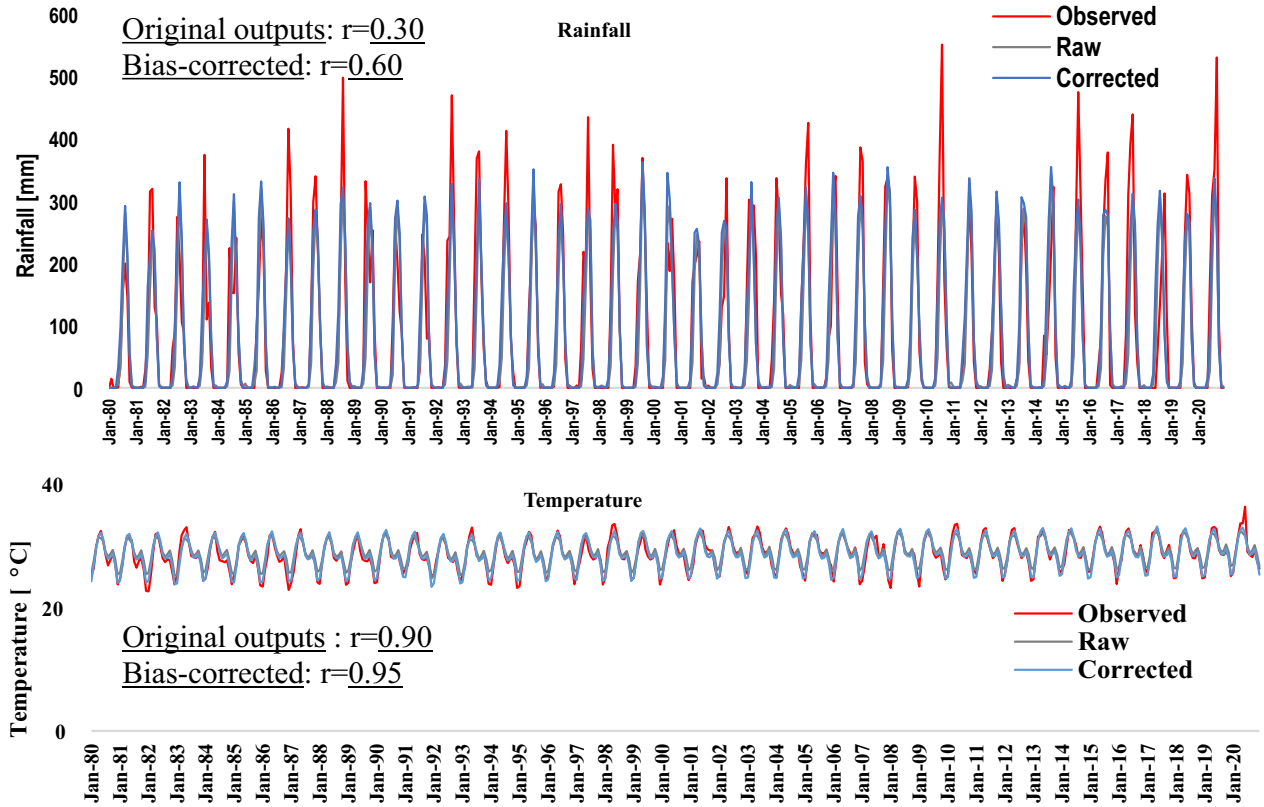

Fig. 4 Comparison between observed, raw, and simulated precipitation and temperature data in the basins

the average values are calculated. Specifically, the study focused on the SSP1-2.6 (low adaptation challenge, low mitigation challenge) and SSP5-8.5 (high mitigation challenge) scenarios [32]. These are two of four Tier 1 scenarios (SSP1-2.6, SSP2-4.5, SSP3-7.0, and SSP5-8.5), designed to provide a full range of forcing targets similar in magnitude and distribution to the RCPs, used in CMIP5. Historical data covering the period 1985–2014 were selected, along with future data spanning the period 2021–2100. Total daily precipitation data from each climate model were used for the analysis. The model simulations were obtained from the data source: (https://esgf-data.dkrz.de/search/cmip6-dkrz/, accessed on March 10, 2023).

These two families of scenarios were thus defined according to the importance of the adaptation and mitigation challenges to be met by societies [77] . SSP1-2.6 (low adaptation challenge, low mitigation challenge) describes a world marked by strong international cooperation, giving priority to sustainable development, very close to the "Proaction" family. SSP5-8.5 (low adaptation challenge, high mitigation challenge) describes a world that focuses on traditional, rapid development of developing countries, based on high energy consumption and carbon-emitting technologies; the increase in the standard of living makes it possible to increase the capacity for adaptation, in particular thanks to the reduction in extreme poverty.

The upcoming forecasts were evaluated over three 20-year periods: near future (2021–2040), medium future (2041–2060), and far future (2081–2100), using the 30-year control period of 1985–2014. The choice of this division into time horizons is explained by the need to generally have three horizons (near, medium and distant), through which hydroclimate trends are studied and compared. The data from the three future horizons (each 20 years long) are compared to that of the 30-year period (1985–2014), a period which constitutes a reference in climatology. The use of 30-year periods as a reference period is based on a scientific statistical convention that a minimum of 30 data points would be required to determine an average. Thus, calculating an average of data over a period of 30 years is the preferred method for representing the average state of a climate. This helps ensure that what is described is actually an aspect of the climate system and not the more variable experience of weather conditions. Annual averages can vary greatly from year to year, whereas a 30-year average eliminates much of this variation and sheds more light on common conditions [103]. The input data for the GR2M model consisted of

bias-corrected future scenarios (the results of the models and the corrected data are evaluated beforehand to ensure the quality of the data), which were used to simulate future runoff. In this study, it was assumed that the precipitation–runoff relationship established from observational time series and the calibrated/validation periods would remain consistent, irrespective of potential land-use changes.

Results and discussion

Modeling over the historical period

Average flows simulated during the calibration and validation phase

The calibration process for the GR2M model was conducted for different time periods in the Casamance and Kayanga basins. In the Casamance basin at the Kolda station, calibration was performed for the period 1981–1986 (the year 1981 (over the 12 months) used as a warm-up period), followed by validation for the period 1987–1992. The results of monthly runoff simulations at the Kolda station are presented in Table 2. The calibration outcomes using the GR2M model demonstrated good quality, with average Nash criteria performance consistently above 60%, except for Nash lnQ, which had a value of 51.5%. The simulation of peak flows (Q) exhibited a very satisfactory performance, as indicated by the Nash value of 70.4%. However, the simulation of low flows (NlnQ) yielded moderately lower results compared to high flows, with a value of 51.5%. The simulation of medium flows (Nash ($\sqrt{Q}$)) also provided good results, with a performance value of 73.4%. In the Kayanga basin at the Wassadou station, calibration was conducted for the period 1985–1988, and validation was performed for the period 1999–2002. The performance in simulating peak flows during the calibration period at Wassadou was relatively lower, with a performance criterion of only 21.5%. However, the performance improved for simulating low flows (Nash (lnQ) = 63.5%) and medium flows (Nash ($\sqrt{Q}$) = 58.9%). Table 2 illustrates the performance metrics. Notably, the performance at Wassadou significantly improved during the validation period, particularly for Nash (Q) and Nash ($\sqrt{Q}$) in percentage values (Table 2).

In the Casamance basin at the Kolda station, the GR2M model is effective in simulating mean and low-water flows over the entire basin on a monthly scale (Fig. 5). On the other hand, the poor performance of the model at the Kolda station and especially at Wassadou, for peak flood flows, can be explained by the poor coverage of this sub-basin with rainfall stations, resulting in a poorly expressed mean value. Figure 5 shows the hyetogram of monthly rainfall and the hydrographs of monthly observed and simulated flows during the calibration period at the Kolda station in the Casamance basin (1981–1986) and at the Wassadou station in the Kayanga basin (1982–1987). For the observed and simulated hydrographs, we have the same signals of variations even

Table 2 Results of calibration and validation of the GR2M model in the Casamance basin in Kolda and the Kayanga basin in Wassadou

Casamance basin in Kolda	Period	Nash (Q)	Nash ($\sqrt{Q}$)	Nash (ln(Q)) in % (ln(Q) in %)	Balance sheet
Calibration	**1981–1986**	**70,4**	**73,4**	**51,5**	**1,18**
Validation	**1987–1992**	**69,0**	**70,3**	**48,4**	**1,09**
Kayanga basin at Wassadou	**Period**	**Nash (Q)**	**Nash ($\sqrt{Q}$)**	**Nash (ln(Q)) in % (ln(Q) in %)**	**Balance sheet**
Calibration	**1985–1988**	21,5	58,9	63,5	**1,40**
Validation	**1999–2002**	83,8	52,4	14,2	**0,87**

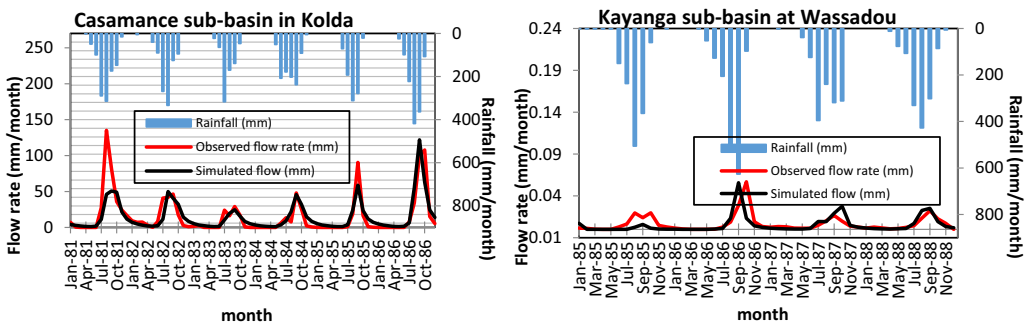

Fig. 5 Hydrographs observed and simulated during the calibration phase by the GR2M model at Kolda in the Casamance basin (1981–1986) and Wassadou in the Kayanga basin (1982–1987)

if the amplitudes differ. In the Casamance basin at the Kolda station, we also note that the peak flows (floods) of 1981 and 1985 were underestimated at the Kolda station with 135 and 63.11 mm/month, respectively (however, the bad performances on the first year in these basins are linked to the warming period). From 1982 to 1984, the observed and simulated flows were similar. In general, the mean monthly water levels calculated reproduce seasonal variations satisfactorily for the calibration sample. However, they vary from year to year.

For the validation period, in the Casamance basin at the Kolda station, the average performance of the Nash criterion was always above 60%. Simulation of peak flow (Q) is also very satisfactory (69%). Simulations of low flows (NlnQ), unlike the peak flow, gave an average result (48.4%). Simulation of medium flows (N($\sqrt{Q}$)) also gave good results (70.3%) (Table 2 and Fig. 6). In the Kayanga basin at the Wassadou station, the simulations for the validation phase are not as good as in Kolda, but they are much better than the results of the calibration phase. This may be due to the quality of the rainfall and flow data used and whose measurements often suffer from errors and uncertainties. The simulated peak flows are well situated in time, but are often underestimated or overestimated. The performances were 83.8% for the Nash (Q), 52.4% for the Nash ($\sqrt{Q}$), and only 14.2% for the Nash (lnQ). While peak flows were poorly reproduced by the model during the calibration phase, during validation, low flows are the least reproduced at the Wassadou station.

Overall, both in calibration and in validation, the shape of the hydrographs observed is well reproduced by the model, and low-water flows are well simulated (with the exception of the results obtained from January 2000 to November 2002 over the validation period in the Kayanga basin). However, the model has difficulty reproducing flood peaks, and there are sometimes significant uncertainties [9]. In general, rainfall is the main driver of flows at the outlet. A number of observations concerning the rainfall-discharge relationship have been made: flood peaks are the consequence of rainfall events, with a more or less significant time lag. This can be explained by a time of concentration (defined as the maximum time required for a drop of water to travel the hydrological path between a point and its outlet) in the Kolda catchment, which varies in length depending on the length of the main watercourse at the location where the rainfall is recorded, the initial humidity conditions in the catchment [47], the lithological conditions in the catchment and, finally, the land use [90].

Table 3 shows the small difference between observed and simulated flows, both for model calibration and for validation, with simulated flows close to, by higher or lower values, than observed flows.

In the Casamance basin at the Kolda station, the simulated mean flow is 14.8 mm in calibration for a mean observed flow of 17.4 mm (with the simulated mean flow < the observed mean flow), whereas in validation, the simulated mean flow is 19.2 mm and the observed mean flow is 17.2 mm (with the simulated mean flow > the

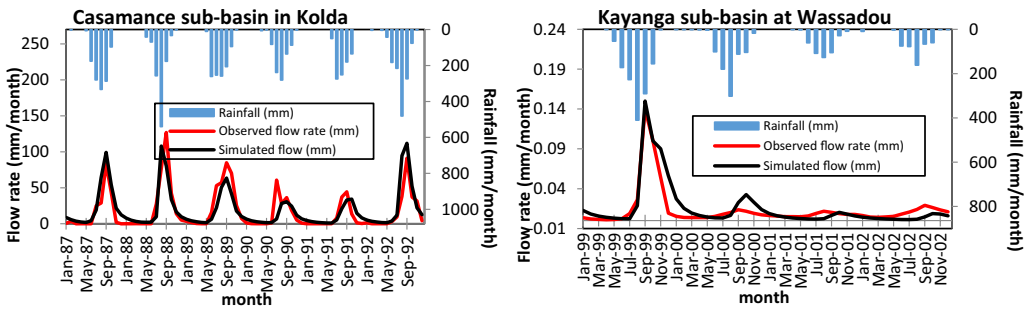

Fig. 6 Hydrographs observed and simulated during the validation phase using the GR2M model at Kolda in the Casamance basin and Wassadou in the Kayanga basin

Table 3 Average flows observed and simulated (mm) by the GR2M model in the Casamance basin at Kolda and the Kayanga basin at Wassadou

Descriptors	Calibration			Validation		
	Observed flow	Simulated flow	Difference	Observed flow	Simulated flow	Difference
Kolda	17,4	14,8	− 2,6	17,6	19,2	1,6
Wassadou	0,007	0,005	− 0,001	0,013	0,015	− 0,002

observed mean flow). Thus, we note a slight underestimation of the water level flowed in calibration (− 2. − 6 mm or − 14.9%), whereas in validation, it is a slight overestimation of the water level flowed (1.60 mm or 9.1%). In the Kayanga basin at the Wassadou station, the simulated mean flow is 0.005 mm in calibration for a mean observed flow of 0.07 mm (with the simulated mean flow < the observed mean flow), whereas in validation, the simulated mean flow is 0.013 mm and the observed mean flow is 0.015 mm (with the simulated mean flow > the observed mean flow). Thus, we note a slight underestimation of the water level flowed in calibration (− 0.001 mm or − 28.6%), whereas in validation, it is a slight overestimation of the water level flowed (0.002 mm or 15.4%).

Figure 7 shows the scatter plots between simulated flows and those observed during the calibration and validation periods at the Kolda station in the Casamance basin and at the Wassadou station in the Kayanga basin. At the Kolda station in the Casamance basin, the performance of the Nash criterion during calibration was always better than that obtained during the validation phase, which was not always the case at Wassadou. The results obtained at the Kolda station show that the flows observed are well reconstructed, both during the calibration phase and the validation one, both for extreme flows (flood and low water), which is not necessarily the case at Wassadou. The correlation between observed flows and simulated flows (Fig. 7) shows better correlation coefficients for calibration than for validation at Kolda and validation for the Wassadou station. However, the results obtained show that the GR2M model is an effective model for simulating monthly flows, especially in the Casamance basin at the Kolda station. The simulated values are close to those observed and attest to the model's validity. In Kolda, a study of the relationship between observed and simulated flows for the 1981–1986 and 1987–1992 sub-periods (Table 4) shows acceptable correlation coefficient values (often greater than 0.60). An adjustment of the scatterplots using linear regression showed that there is a good correlation between simulated and observed flows, with a correlation coefficient r equal to 0.81 in calibration (1981–1986) and 0.84 in validation (1987–1992) at Kolda in the Casamance basin. In the Kayanga basin at the Wassadou station, the correlation coefficient r is equal to 0.59 in calibration (1985–1988) and 0.92 in validation (1999–2002) (Table 5)

The uncertainties and robustness of the GR2M model

Analysis of the different performances (**5**) first shows that calibration performance is better than validation

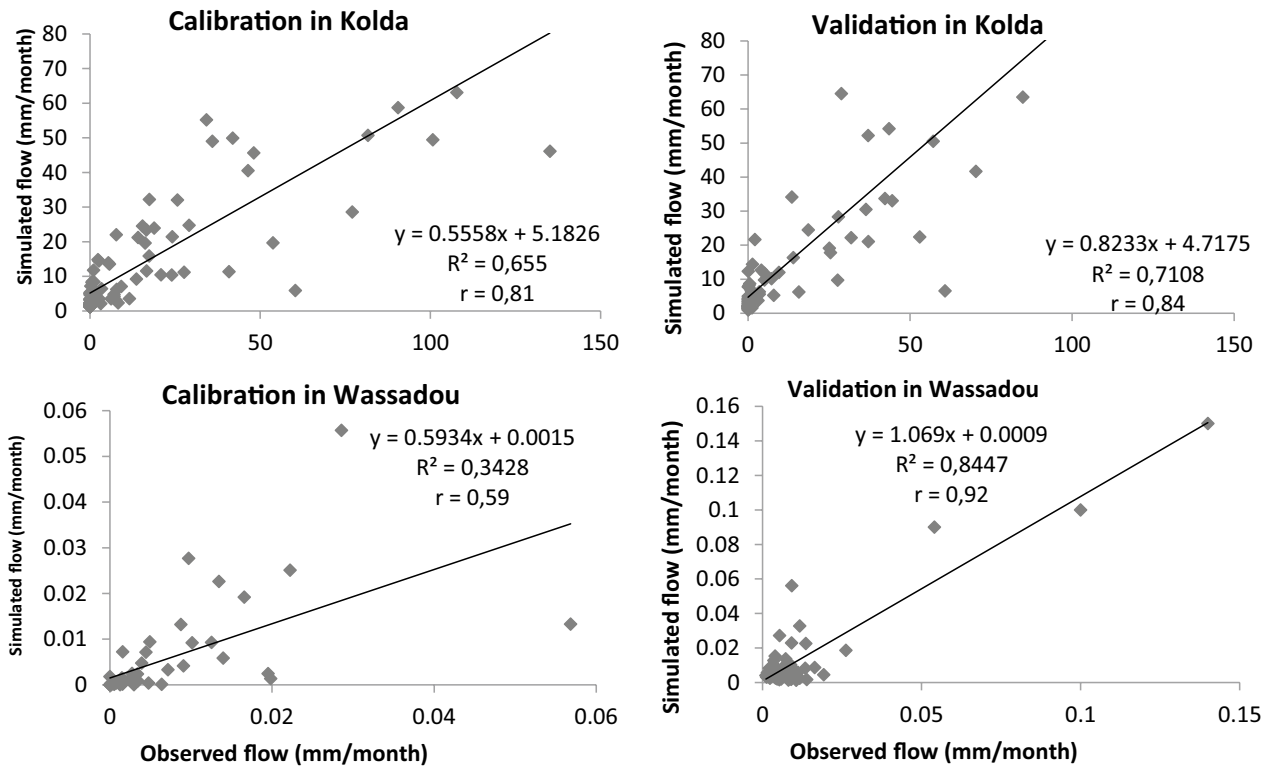

Fig. 7 Correlation between observed flows and flows simulated during calibration and validation by GR2M in the Casamance basin at Kolda and the Kayanga basin at Wassadou

Table 4 Correlation between observed and simulated flows in calibration and validation in the Casamance basin at Kolda and the Kayanga basin at Wassadou

Station	Correlation coefficient for calibration	Correlation coefficient in Validation
Kolda	0,81	0,84
Wassadou	0,59	0,92

If the coefficients are on an interval of 0.3 to 1, the correlation is considered positive and strong

performance. Second, it can be seen that performance over the calibration period (1981–1986 with 65.1%) is better than that over the validation period (1987–1992 with 62.6%) at the Kolda station in the Casamance basin. At Wassadou, in the Kayanga basin, average performance, which was 48% in the calibration period (1985–1988), improved slightly in the validation period (1999–2002), with a value of 50.2%.

Overall, the results obtained with the GR2M model are satisfactory in the Casamance basin upstream of Kolda. The Nash criterion generally performs better than 60% in calibration and validation. The GR2M model provides a satisfactory representation of the relationship between the estimated mean monthly rainfall in the Casamance basin upstream of Kolda and the mean monthly discharge recorded at its outlet (which is not necessarily the case at Wassadou). The number of parameters is the same in the two basins, making the model robust. However, there are still limitations in the modeling of the rainfall–runoff relationship, and the associated uncertainties are shown in Table 6. These uncertainties in calibration and validation are given by the ratio between the observed flows for each month and the simulated flows for that month.

These uncertainties over each period are given by the ratio between the flow rates observed over each month and the simulated flow rate for the same month, during the calibration and validation period.

In the Casamance basin at the Kolda station, the errors are generally around 0 to 9 mm, although there are a few that are further away (9.65 in calibration and 9.45 in validation). Low flows are sometimes twice underestimated or overestimated. High flows, on the other hand, are only slightly underestimated. The simulated flows, despite some uncertainty, are on the whole acceptable, having regard to the Nash criteria. An analysis of the variation in the parameters of the GR2M model enables us to appreciate the role played by the underground reservoirs in the hydrological dynamics of the basin. In the Kayanga basin at the Wassadou station, these mean errors are 2.77 in calibration (1985–1988) and 1.78 in validation (1999–2002). In the Casamance basin at Kolda and the Kayanga basin at Wassadou, in both calibration and validation, the worst Nash criterion performances were obtained with the lowest values of *X1* and *X2*, whereas the best performances were obtained with the highest values of *X1* and *X2*. The GR2M model appears to be more sensitive to variations in *X1* than in *X2*. In the same way as rainfall, soil water capacity is an essential input for the model to work properly. In both calibration and validation, the delays and advances (lags) in the simulated hydrographs are largely explained by the poor simulation of the end of the rainy seasons, which, in the case of deficit years, is greatly underestimated. On the other hand, in surplus years, where the response to high rainfall concentration at the end of the season is still poorly reproduced by the model, it is greatly overestimated [49]. A study of the parameters of the GR2M model (*X1* and *X2* values are often low) shows that the various sub-basins studied have "soil" reservoirs that do not have very large reserve capacities, which indicates that the recharge and support of underground reserves in the various sub-basins is weak. In general, the monthly time step is a relevant scale for simulating flows in the Casamance basin in Kolda and the Kayanga basin in Wassadou in a context of climate variability and change. When the model's performance shows good calibration and validation characteristics, as was the case for the Casamance basin upstream of Kolda, the parameters can be applied for series under climate change, as demonstrated by Okkan and Fistikoglu [74]. Thus, for future simulations with GR2M, the Casamance basin upstream of Kolda will have the best results, because the performance of the GR2M model is considered sufficient (the model is excellent there, because Nash is between 0.6 and 0.8 for both calibration

Table 5 Average robustness criteria of the GR2M model in the Casamance basin at Kolda and the Kayanga basin at Wassadou

Descriptors	Average performance (calibration)	Average performance (validation)	Average performance	Variation % change
Kolda	**65,1**	**62,6**	**63,8**	**2,9**
Wassadou	**48,0**	**50,1**	**49,1**	**0**

The average performance used here is the average value of the three types of Nash used (Nash (Q), Nash ($\sqrt{Q}$), and Nash (ln(Q)))

Table 6 Average uncertainties during the calibration and validation phases in the Casamance basin in Kolda and the Kayanga basin in Wassadou

Descriptors	Calibration uncertainties	Uncertainties in validation
Kolda	**9,65**	**9,45**
Wassadou	**2,77**	**1,78**

and validation). For the Kayanga basin, which does not meet this principle (the model is inadequate, because Nash < 0.22 in the calibration phase), future modeling has been carried out with GR2M for this basin, but the data are used just to illustrate the analysis of future flows in the Casamance basin upstream of Kolda.

Modelling for the future period

The impact of climate change on future runoff in the upstream area of the Casamance basin, specifically upstream of Kolda, was assessed using the GR2M model. Two different climate change scenarios based on the Shared Socioeconomic Pathways (SSPs) were considered. SSP1 represents a future with low mitigation and adaptation challenges, SSP3 assumes high population growth and low economic development, while SSP2 and SSP5 fall in between with varying characteristics. The hydrological modeling techniques utilized General Circulation Models (GCMs) and their ensemble mean to analyze historical and projected trends in hydroclimatic parameters. Precipitation and potential evapotranspiration data under SSP1-2.6SSP1-2.6 and SSP5-8.5 scenarios were used in the GR2M model to generate mean runoff rates for the upcoming decades in the region. These analyses help understand the potential impacts of climate change on future flow patterns in the Casamance basin upstream of Kolda.

Precipitation and temperature trends from 2021 to 2100

Over the period 2021–2100, a decrease in precipitation would be noted for the SSP1-2.6 and SSP5-8.5 scenarios of the order of − 0.2 mm per year and − 0.687 mm per year, respectively. This trend is corroborated by the Pettitt test (Table 7), which shows a break in the prospective precipitation series in 2065 and 2052 respectively for the SSP1-2.6 and SSP5-8.5 climate change scenarios over the study period (2021–2100). On either side of the break date, there is a decrease of around 4.1 and 17.9%, respectively, for the SSP1-2.6 and SSP5-8.5 climate change scenarios.

For the 2030 climate horizon (2021–2040 period), precipitation should increase slightly, as indicated for the SSP1− 2.6 and SSP5-8.5 scenarios, by around 0.147 and 0.021 mm per year, respectively. On the other hand, for the 2050 (2041–2060) and 2070 (1961–2080) horizons, a decrease in precipitation would also be noted for the SSP1-2.6 and SSP5-8.5 scenarios. This decrease would be of the order of − 0.147 mm per year for the SSP1-2.6 scenario and − 0.505 mm per year for the SSP5-8.5 scenario over the 2050 horizon (2041–2060), and of the order of − 0.274 mm per year for the SSP1-2.6 scenario and -0.116 mm per year for the SSP5-8.5 scenario over the 2070 horizon (1981–2100). For the 2090 horizon (1981–2100), the situation would be disparate, with an increase of around 0.158 mm per year for the SSP1-2.6 scenario, while for the SSP5-8.5 scenario, a decrease in precipitation of around − 0.295 mm per year would be noted. The decrease in rainfall is confirmed in the Kayanga basin upstream of Wassadou, with a decrease of around -0.2 mm under the SSP1-2.6 scenario and -0.627 mm under the SSP5-8.5 scenario (Table 7). The observed trend of decreasing annual precipitation in the Casamance and Kayanga-Géva basins is highly variable. However, the location of these basins and the evidence of precipitation variability align with the projections of the Intergovernmental Panel on Climate Change [27, 28]. These changes in precipitation patterns are attributed to shifts in continental and sea surface temperatures, along with variations in wind patterns and ocean currents. The observed variability in precipitation is consistent with the other studies that have predicted reductions in rainfall over West Africa.

Table 7 Variation in rainfall and mean annual temperature over the future period (2021–2100) compared with the historical period (1985–2014) at the Kolda and Wassadou stations

Rainfall	Casamance in Kolda		Kayanga in Wassadou	
	SSP1-2.6	SSP5-8.5	SSP1-2.6	SSP5-8.5
2021–2040	− 7,90	2,64	− 6,4	2,3
2041–2060	− 6,11	− 7,77	− 5,2	− 7,7
2061–2080	− 9,25	− 16,31	− 8,4	− 15,6
2081–2100	− 10,97	− 22,15	− 9,0	− 21,2
2021–2100	− 8,61	− 11,04	− 7,2	− 10,6
Temperature	SSP1-2.6	SSP5-8.5	SSP1-2.6	SSP5-8.5
2021–2040	1,43	1,18	1,59	1,29
2041–2060	1,80	2,43	1,98	2,53
2061–2080	2,09	3,77	2,25	3,87
2081–2100	1,98	5,20	2,12	5,31
2021–2100	1,84	3,18	1,99	3,25

For temperatures, this upward trend remains generally constant for the four time horizons 2030, 2050, 2070, and 2090 and for both scenarios. For scenario 126, this rise in temperatures at the Kolda station is, respectively, of the order of 0.589, 0.347, and 0.116 °C/year for the 2030, 2050, and 2070 horizons, while for the 2090 horizon, a fall of − 0.28 °C/year will be noted. For scenario 585, this generalized rise in temperatures would be of the order of 0.874, 0.905, 0.842, and 0.811 °C/year for the 2030, 2050, 2070, and 2090 horizons, respectively (Table 7). This trend toward higher temperatures leads to an increase in potential evapotranspiration, which has an impact on water availability in the basin. The Casamance basin is located in a region with high climatic variability and

historical increases in temperature. This is also the case for the Kayanga basin at the Wassadou station (Table 7), where there is a decrease in rainfall (− 7.2% for SSP1-2.6 and − 10.6% for SSP5-8.5) and an increase in temperature (1.99 °C for SSP1-2.6 and 3.25 °C for SSP5-8.5), if the future period is compared with the historical period. Compared with the historical period (1985–2014), a general decrease in rainfall and a general increase in temperature over the four horizons studied would be noted in the Casamance basin at Kolda (Table 7). This decrease in rainfall over the 2030, 2050, 2070, and 2090 climate horizons, compared with the historical period, could reach values of 7.90, 6.11, 9.25, and 10.97%, respectively in the SSP1-2.6 scenario, and 7.77, 16.31, 22.15, and 11.04%, respectively, over the 2050, 2070, and 2090 horizons in the SSP5-8.5 scenario. Temperatures could rise by a record 2.09 °C over the period 2061–2080 in the SSP1-2.6 scenario and 5.20 °C over the period 2081–2100 in the SSP5-8.5 scenario.

Changes in runoff from 2021 to 2100

Figures 8, 9, 10 and 11 illustrate the changes in monthly and annual mean flows for the Kolda station in the Casamance basin and the Wassadou station in the Kayanga basin under the SSP1-2.6 and SSP5-8.5 scenarios for the time horizons of 2030, 2050, 2070, and 2090. These basins are situated in the West African region, and the observed hydroclimatic variability aligns with the projections of the Intergovernmental Panel on Climate Change. The models indicate a decrease in mean monthly flows in the future for both scenarios and across all four time horizons at these stations. These findings suggest that surface water resources in these catchment areas are expected to continue declining throughout the twenty-first century, particularly under the SSP5-8.5 scenario. The Casamance sub-basin in Kolda and the Kayanga sub-basin in Wassadou remain highly susceptible to climate change due to the greater reduction in rainfall. For the Casamance basin at the Kolda station, the SSP1-2.6 climate scenario forecasts a mean future discharge of 2.73 mm. The application of the Mann–Kendall test to the discharge series reveals a downward trend, which is supported by the Pettitt test. This trend shows a break in 2053 for the 2050 climate horizon, with an average discharge of 2.84 mm before the break and 2.41 mm after the break, representing a deficit of 15.25% (Fig. 8). Under the SSP5-8.5

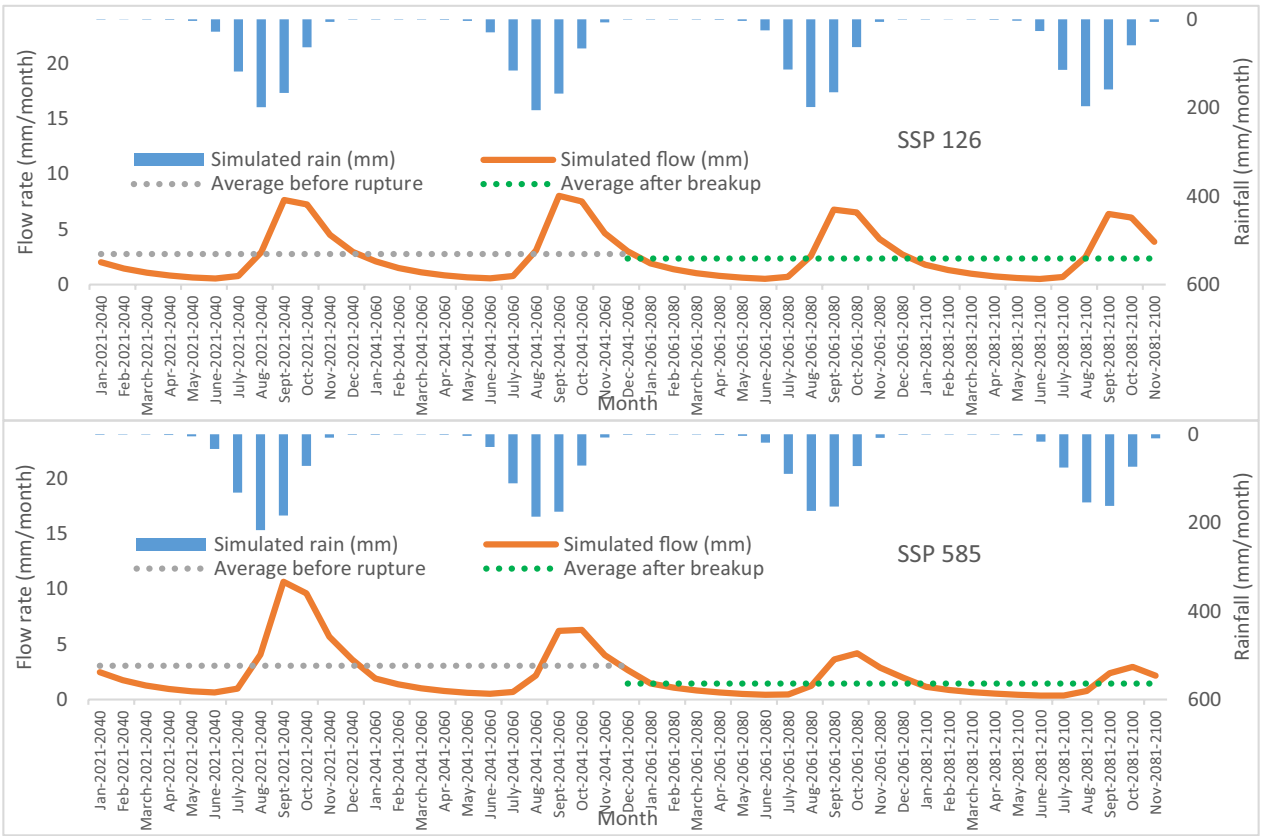

Fig. 8 Variation in future flow simulated by the GR2M model for the period 2021–2100 at the Kolda station in the Casamance basin, according to the SSP1-2.6 and 585 climate change scenarios for the periods 2021–2040, 2041–2060, 2061–2080, and 2081–2100

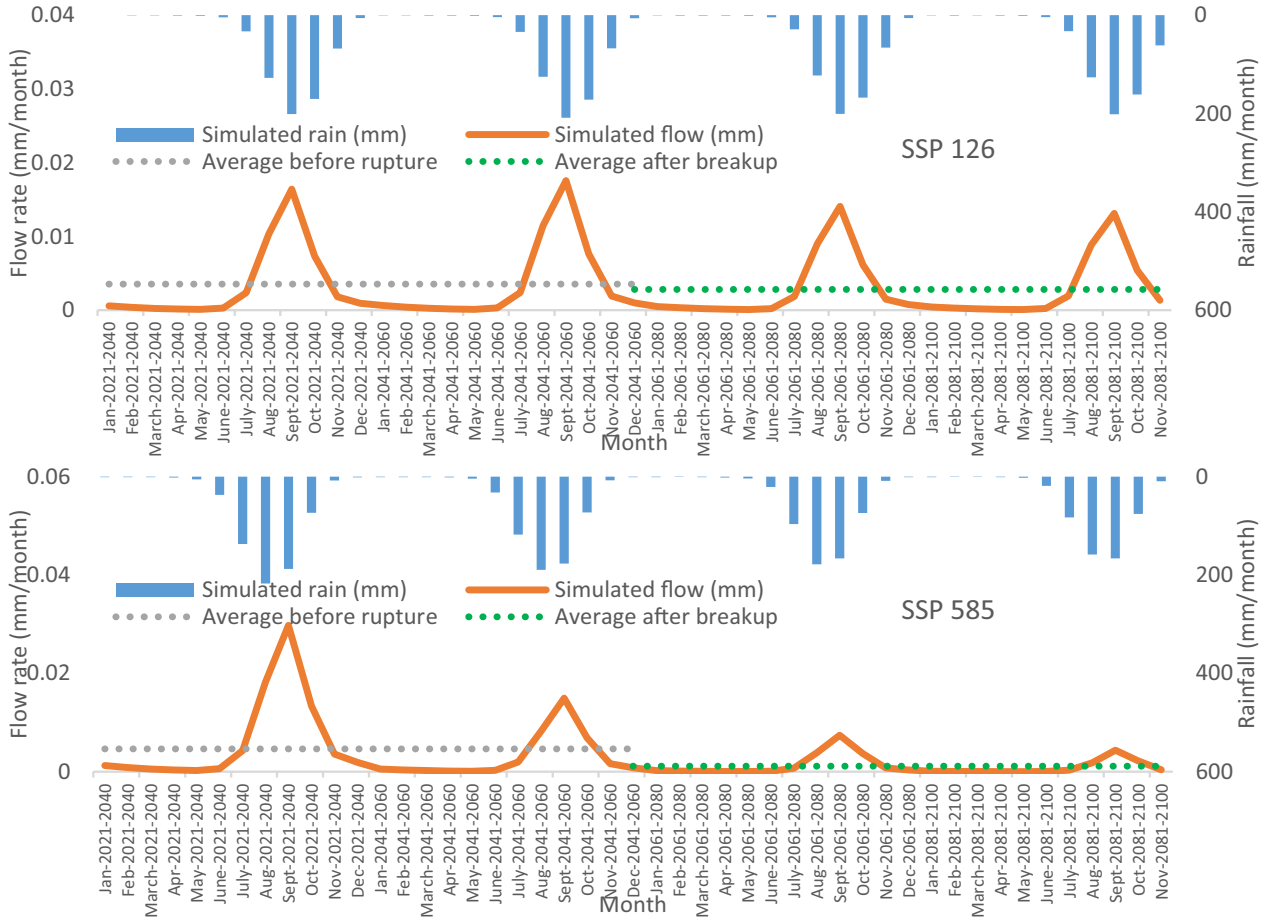

Fig. 9 Variation in future flow simulated by the GR2M model for the period 2021–2100 at the Wassadou station in the Kayanga-Géva basin, according to the SSP1-2.6 and 585 climate change scenarios for the periods 2021–2040, 2041–2060, 2061–2080, and 2081–2100

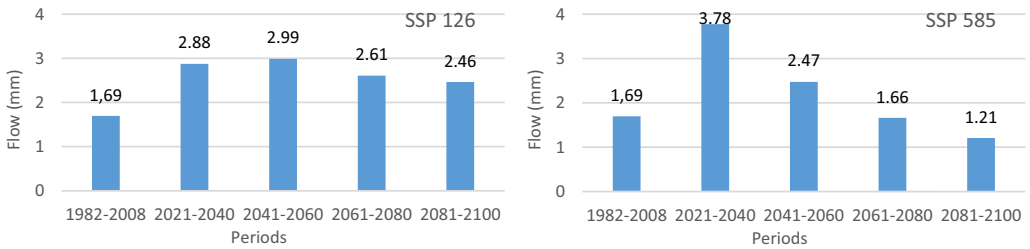

Fig. 10 Comparison between the observed mean historical flow and the flow simulated in the SSP1-2.6 and 585 climate change scenarios for the future period at the Kolda station

climate change scenario, the expected mean discharge is 2.26 mm, and the break in the flow series occurs in 2056 for the 2050 time horizon. The average discharge before the break is 3.06 mm, while after the break, it drops to 1.44 mm, resulting in a flow deficit of 52.76% (Fig. 8). In the Kayanga basin at the Wassadou station, the runoff projected under the SSP1-2.6 climate scenario indicates an average runoff of 0.003 mm. The analysis shows a break occurring in 2054 for the 2060 time horizon, with an average runoff of 0.0036 mm before the break and 0.0028 mm after the break, indicating a deficit of 22.61% (Fig. 9). For the SSP5-8.5 scenario, the break occurs in 2060, with a mean discharge of 0.0029 mm. Before the break, the average runoff is 0.0046 mm, but after the

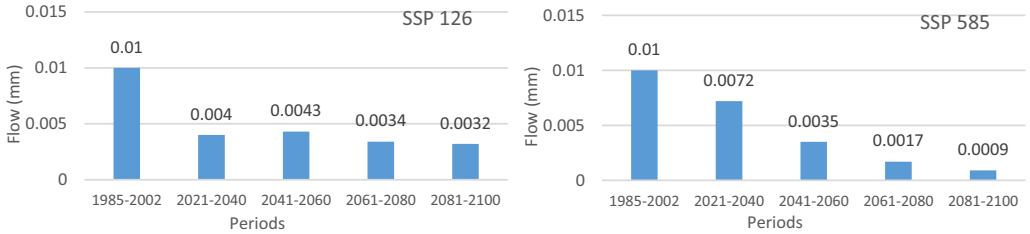

Fig. 11 Comparison between the observed mean historical discharge and the simulated discharge under the SSP1-2.6 and 585 climate change scenarios for the future period at the Wassadou station

break, it reduces significantly to 0.0011 mm, representing a drop of 75.85% (Fig. 8). These results highlight the considerable changes in flow patterns expected in the Casamance and Kayanga basins under different climate change scenarios, emphasizing the urgency of adapting water resource management strategies to mitigate the potential impacts of decreased water availability.

The historical discharge observed at the Kolda station in the Casamance basin was relatively low, with an average of 1.69 mm over the period from 1982 to 2008. This period coincided with a drought, which resulted in decreased flows in the basin. Due to this drought period, the observed discharge falls below the average flows simulated for the different periods (2021–2040, 2041–2060, 2061–2080, and 2081–2100) or horizons (2030, 2050, 2070, and 2090) (Fig. 10). Consequently, it becomes challenging to directly compare the observed discharge with the simulated flows. However, when comparing the near-future horizon (2021–2040) with the 2070 and 2090 horizons under the SSP1-2.6 climate scenario, a downward trend is projected. The simulated flows show a decrease of -9.25% and -14.34%, respectively, for these future horizons. In contrast, an increase is projected for the 2050 horizon, with a value of 3.98% (Fig. 11). These findings suggest potential changes in the flow patterns of the Casamance basin in the coming decades, indicating a potential shift toward decreased discharge under certain climate scenarios.

According to the SSP5-8.5 scenario, there is a projected overall decline in flow compared to the simulated flow for the period 2021–2040 in the Casamance basin. The decline percentages for each climate horizons (2050, 2070, and 2090) are − 34.47%, − 56.01%, and − 68.01%, respectively (Fig. 10). This decline in water resources under the SSP5-8.5 scenario is a matter of concern, considering the challenging climate change conditions in the basin, especially when compared to the SSP1-2.6 scenario. In the Wassadou station, which is located in Kolda, the observed average historical discharge over the period 1985–2002 is only 0.01 mm, higher than the average discharges simulated for various periods (2021–2040, 2041–2060, 2061–2080, and 2081–2100) or climate horizons (2030, 2050, 2070, and 2090) (Fig. 11). Under the SSP1-2.6 climate scenario, a downward trend is expected for the 2030, 2050, 2070, and 2090 horizons, with decline percentages of − 60%, − 57%, − 66%, and − 68%, respectively, compared to the historical period. For the SSP5-8.5 scenario, there is a general decline compared to the historical period, with decline percentages of − 28%, − 65%, − 83%, and − 91% for the successive periods. These findings indicate a worrisome trend of declining water resources in the Casamance basin, particularly under the SSP5-8.5 scenario. It highlights the urgent need to address the challenges posed by climate change and adapt water management strategies to mitigate the potential impacts of decreasing water availability.

Discussion

Modeling the rainfall–discharge relationship has provided valuable insights into the hydrological behavior of the Casamance basin at Kolda and the Kayanga-Géva basin. The results demonstrate satisfactory performance of the hydrological model in reproducing flows at the outlet of the Casamance basin at Kolda. The good fit between observed and simulated flows, as indicated by the Nash criteria and the coefficient of determination (R2), further validates the model's capability to realistically represent the flow dynamics [46]. The hydrological model successfully captures the hydrological regimes of the basins, consistent with previous studies by Khoulé [47]. Interestingly, despite being developed for a specific type of climate, the application of the model in the Casamance basin at Kolda (not generally the case in the Kayanga basin at Wassadou), characterized by a southern Sudanian climate, yields acceptable results even in significantly different climatic contexts compared to its original design [55, 85]. Although the two basins are in the same climatic context and there is no significant difference between them, the worst performance of GR2M in Kayanga is more linked to a data problem, but also to the impacts of the Niandouba dams and the Confluent on the measured flow rates (because dams are not take into account in global models like GR2M). Looking toward the future, the models used in this study indicate

a reduction in water resources, particularly toward the end of the century, for both basins. These findings align with similar studies conducted in other regions, particularly when considering the extreme scenarios of CMIP6 [33, 97]. Since rainfall is the primary driver of runoff in the Casamance basin, changes in seasonal rainfall distribution in climate models directly impact runoff patterns. Consequently, the seasonal variations in runoff closely follow those of rainfall [46]. It is important to note that the results are heavily influenced by the global hydrological model used (GR2M), which is relatively simple and operates with two parameters. Utilizing a distributed hydrological model could potentially enhance these results. Overall, the hydrological modeling approach employed in this study provides valuable insights into the future water availability in the Casamance and Kayanga-Géva basins. However, further refinements, such as employing a distributed hydrological model, can be explored to improve the accuracy and precision of the projections.

Climate change models have predicted a reduction in annual runoff in major water-producing basins across West Africa, leading to increased drought frequency and decreased surface runoff [87]. These changes are expected to have a detrimental impact on water availability for urban and agricultural sectors. Climate change has already been observed to negatively affect crop productivity, with increased temperatures leading to shorter growing periods and temperatures beyond the optimal range for plant development [29, 74]. Consequently, it is crucial to take action to minimize water losses and enhance water use efficiency, especially in sectors with high demand. Measures such as promoting low-water content and heat stress-tolerant crops, employing good tillage practices to maintain soil moisture, and implementing advanced irrigation techniques have been encouraged to mitigate the consequences of climate change on agriculture [91]. The population in the Kolda region heavily relies on surface water runoff from the Casamance and Kayanga basins for surface irrigation through canals, particularly in the Anambé basin. Climate change will significantly impact the ecological biodiversity of the basin as the resilience capacity of the ecosystem will be exceeded by reduced surface flows, affecting various flora and fauna species that depend on upstream water runoff for their survival [25]. Overall, the three climate change scenarios indicate a decrease in average monthly flows across different time horizons and scenarios, with a greater reduction observed under the SSP5-8.5 scenario compared to the SSP1-2.6 scenario. The decline is particularly pronounced during the wettest months (June, July, August, and September), while minor increases may be observed in less rainy months. Studying the impact of climate change on water resources is a significant challenge. Optimal management of water resources in terms of quantity and quality is essential for sustainable development in Senegal. The primary objective of this study was to provide insights into the potential impacts of climate change on future flow changes in the Casamance basins upstream of Kolda, utilizing the GR2M model. Hence, the outputs from climate models under the SSP1-2.6 and SSP5-8.5 scenarios were used as inputs for the GR2M hydrological model to simulate flows up to 2060.

It is important to note that precipitation and runoff simulations vary across different regions due to regional climate characteristics, uncertainties in global boundary conditions and greenhouse gas scenarios, physical parameterization schemes, and algorithms. Therefore, differences in precipitation simulation between regions and scenarios are reflected in runoff. Generally, both climate change scenarios indicate peak flows in September. However, significant decreases and alterations in the seasonal flow cycle are observed in all scenarios, primarily driven by changes in the precipitation regime in terms of frequency and intensity [40].

Climate modeling induces many uncertainties in climate analysis. It is necessary to be aware of this and take it into account to best understand the data from model outputs, as well as for the interpretation of indicators of possible changes in the future climate [3]. The first uncertainties relate to the models used. In fact, they are based on past data measured in situ. However, the quality of this measured data varies. The data regionalization method also induces statistical approximations and uncertainty persists in the modeled data despite the corrections made. There are also uncertainties linked to climate change scenarios.

Finally, uncertainties linked to the lack of knowledge about certain processes exist. Indeed, the carbon cycle process is still poorly understood, particularly in relation to aerosols.

There is also the coarse resolution of GCMs (~ 200 km) which cannot capture local climatic features in small watersheds.

Furthermore, using the average ensemble alone will certainly make it possible to circumvent the divergence of the climate model for the future horizon, but this will mask the uncertainties about the future climate.

Conclusion

This paper designed to model the rainfall–discharge relationship with understand hydrological behavior in the Casamance catchment at Kolda and the Kayanga-Géva catchment. The GR2M model was chosen for its advantages in terms of little data necessities, basic arrangement,

high show, and computational efficiency. By utilizing model, native authorities can kind conversant decisions and plan water resource management, considering the challenges posed by climate change. The emphasis was on examining the effects of climate variation on flow characteristics in West African tropical catchments. Historical outputs presented that GR2M model effectively simulated precipitation and temperature cycles in the catchments. However, biases existed between the outputs of General Circulation Models (GCMs) and observed data. Bias correction techniques were applied to obtain more reliable projections. Results indicated important fluctuations in periodic rainfall and temperature distribution for entire watersheds, with decreased rainfall volumes projected for the distant future. Using the future bias-corrected simulations to drive the GR2M model, the study found that surface runoff responses would vary across different future periods and catchment domains, primarily influenced by projected precipitation. Wet conditions in the near future led to higher inter-annual runoff volumes, while drier situations in the distant future resulted in significantly lower runoff volumes. These findings highlight the possible effect of climate change on surface runoff and the need for adaptation policies. The study's results will assist local water management authorities in decision-making regarding climate change impacts on surface runoff, ensuring ecological and financial sustainability. The methodology employed can be applied to similar climatic regions, but further research is necessary to explore various hydrological models, parameter optimization techniques, performance measures, and the effectiveness of water conservation measures.

Acknowledgements
The authors acknowledge the financial support through the Researchers Supporting Project number (RSPD2023R724), King Saud University, Riyadh, Saudi Arabia.
The authors declare that the work described has not been published previously and not under consideration for publication elsewhere. The publication is approved by all authors and tacitly or explicitly by the responsible authorities where the work was carried out.

Author contributions
CAASS: Writing—original draft writing, conceptualization, formal analysis, methodology, data curation, processing of data, development of models, writing—review and editing, and investigation. CF: supervision, writing original draft writing, validation, investigation, methodology, and writing—review and editing. CBP: formal analysis, validation, writing original draft writing, formal analysis, and writing— review and editing. ADT: writing—review and editing, formal analysis, and management, MSA: writing—review and editing, MMSC-P: writing—review and editing, and ME: writing—review and editing.

Funding
Not applicable.

Availability of data and materials
Data will be made available on reasonable request.

Declarations

Ethics approval and consent to participate
Not applicable.

Consent for publication
Not applicable.

Competing interests
The authors declare no competing interests.

Author details
[1]Department of Geography, U.F.R. Sciences Et Technologies, Laboratory of Geomatics and Environment, Assane Seck Univesity of Ziguinchor, BP 523, Ziguinchor, Senegal. [2]New Era and Development in Civil Engineering Research Group, Scientific Research Center, Al-Ayen University, Thi-Qar, Nasiriyah 64001, Iraq. [3]Institute of Energy Infrastructure, Universiti Tenaga Nasional, 43000 Kajang, Malaysia. [4]Indian Institute of Tropical Meteorology, Pune, India. [5]School of Water Resources and Environmental Engineering, Haramaya Institute of Technology, Haramaya University, P.O. Box 138, Dire Dawa, Ethiopia. [6]Department of Chemistry, College of Science, King Saud University, P.O. Box 2455, 11451 Riyadh, Saudi Arabia. [7]Geobiotec Research Centre, Department of Geoscience, University of Aveiro, 3810-193 Aveiro, Portugal. [8]Civil Engineering Department, Faculty of Engineering, Aswan University, Aswan 81542, Egypt.

Received: 11 July 2023 Accepted: 3 December 2023
Published online: 15 December 2023

References

1. Akinsanola AA, Zhou W (2019) Projections of West African summer monsoon rainfall extremes from two CORDEX models Clim. Dyn 52:2017
2. Alamou EA, Obada E, Afouda A (2017) Assessment of future water resources availability under climate change Scenarios in the Mékrou Basin. Benin Hydrology 4:51
3. Amiot, L. (2021) Diagnostic climatique territorial focus « ressource en eau » Guide méthodologique, Publication Juillet, 146 p
4. Ardoin-Bardin S, Dezetter A, Servat E, Paturel JE, Mahé G, Niel H, Dieulin C (2009) Using general circulation model outputs to assess impacts of climate change on runoff for large hydrological catchments in West Africa. Hydrol Sci J 54:77–89
5. Ayugi B, Tan G, Ruoyun N, Babaousmail H, Ojara M, Wido H, Mumo L, Ngoma NH, Nooni IK, Ongoma V (2020) Quantile Mapping Bias Correction on Rossby Centre Regional Climate Models for Precipitation Analysis over Kenya. East Africa Water 12:801
6. Bai Y, Liu H, Huang B, Wagle M, Guo S (2016) Identification of environmental stressors and validation of light preference as a measure of anxiety in larval zebrafish. BMC Neurosci 17:63
7. Bendaoud, H. Modélisation pluie-débit par le modèle conceptuel GR2M : cas du bassin versant de l'oued zeddine, Université SAAD DAHLEB –BLIDA 1, Faculté de Technologie, Département des Sciences de l'Eau et Environnement, Mémoire, 2017, 59 p.
8. Beven KJ (2001) How far can we go in distributed hydrological modelling? Hydrol Earth Syst Sci 5:1–12
9. Bodian A, Dezetter DH (2012) Apport de la modélisation hydrologique pour la connaissance de la ressource en eau : application au haut bassin du fleuve Sénégal. Revue de Climatologie 9(2012):109–125
10. Bodian A, Dezetter A, Diop L, Deme A, Djaman K, Diop A (2018) Future climate change impacts on streamflows of two main West Africa River Basins: Senegal and Gambia. Hydrology 5(1):21. https://doi.org/10.3390/hydrology5010021
11. Bouabdelli S, Meddi M, Zeroual A, Alkama R (2020) Hydrological drought risk recurrence under climate change in the Karst Area of Northwestern Algeria. J Water Clim Change 11:164–188
12. CILSS. (2016). Comité permanent inter-états de Lutte contre la Sécheresse dans le Sahel; landscapes of West Africa-A window on a changing

world: Ouagadougou (Tech. Rep.). 47914 252nd St, Garretson, SD 57030, United States. U.S. Geological Survey EROS
13. Calvo-Valverde L-A, Imbach P, Maathuis B, Hein-Grigg D, Hidalgo-Madriz J-A, Alvarado-Gamboa L-F (2022) Hydrological response of tropical catchments to climate change as modeled by the GR2M model: a case study in costa rica. Sustainability 14:16938. https://doi.org/10.3390/su142416938
14. Clark MP, Slater AG, Rupp DE, Woods RA, Vrugt JA, Gupta HV, Wagener T, Hay LE (2008) Framework for understanding structural errors (FUSE): a modular framework to diagnose differences between hydrological models. Water Res. https://doi.org/10.1029/2007WR006735
15. Clark MP, Wilby RL, Gutmann ED, Vano JA, Gangopadhyay S, Wood AW, Fowler HJ, Prudhomme C, Arnold JR, Brekke LD (2016) Characterizing uncertainty of the hydrologic impacts of climate change. Curr Clim Change Rep 2(2):55–64
16. Culley S, Noble S, Yates A, Timbs M, Westra S, Maier HR, Giuliani M, Castelletti A (2016) A bottom-up approach to identifying the maximum operational adaptive capacity of water resource systems to a changing climate. Water Resour Res. https://doi.org/10.1002/2015WR018253
17. Dacosta, H. Juillet (1989) : Précipitations et écoulements sur le bassin de la Casamance, Thèse de doctorat, Université de Cheikh Anta Diop, Dakar, faculté des lettres et sciences humaines, Département de géographie
18. Dechemi N, Benkaci T, Issolah A (2003) « Modélisation *des débits mensuels par les modèles conceptuels et les systèmes neuro-flous* » Revue des sciences de l'eau. J Water Sci 16(4):407–424
19. Dezetter A, Girard S, Paturel JE, Mahé G, Ardoin-Bardin S, Servat E (2008) Simulation of runoff in West Africa: is there a single data-model combination that produces the best simulation results? J Hydrol. https://doi.org/10.1016/j.jhydrol.2008.03.014
20. Donevska K, Panov A (2019) Climate change impact on water supply demands: case study of the city of Skopje. Water Supply 7:2172–2178
21. Duan Q, Sorooshian S, Gupta VK (1992) Effective and efficient global optimization for conceptual rainfall runoff models. Water Resour Res 24:1163–1173
22. Duminda P, Seidou O, Agnihotri J, Mehmood H, Rasmy M (2020) Challenges and technical advances in flood early warning systems (FEWSs) flood impact mitigation and resilience enhancement. IntechOpen. https://doi.org/10.5772/intechopen.93069
23. Fang Y, Wang H, Fang P, Liang B, Zheng K, Sun, Q.,... Wang, A. (2023) Life cycle assessment of integrated bioelectrochemical-constructed wetland system: environmental sustainability and economic feasibility evaluation. Resour Conserv Recycl 189:106740. https://doi.org/10.1016/j.resconrec.2022.106740
24. Faye C, Sow AA, (2014) Analyse de la variabilité des ressources en eau dans le bassin de la Falémé par modélisation hydrologique, 14 12, 9
25. Food and Agriculture Organization. Consequences of Climate Change. 2013. Available online: http://www.fao.org/3/i2498s/i2498s04.pdf accessed on 5 Feb 2021
26. Fowler K, Coxon G, Freer J, Peel M, Wagener T, Western A, Woods R, Zhang L (2018) Simulating runoff under changing climatic conditions: a framework for model improvement. Water Resour Res 54:9812–9832
27. GIEC. Climate Change 2007. Synthesis Report. Contribution of Working Groups I, II and III to the Fourth Assessment Report of the Intergovernmental Panel on Climate Change. Suiza. 2007.
28. GIEC 2019 Special Report on the Impacts of Global Warming of 15 °C Relative to Pre-Industrial Levels and Corresponding Trajectories that Global Greenhouse Gas Emissions Should Follow, in the Context of Strengthening the Global Response to the Threat Climate Change Sustainable Development and Efforts to Eradicate poverty OMM-PNUMA IPCC Geneva Switzerland
29. Gadgil D (1995) Climate change and agriculture: an Indian perspective. Curr Sci 9:649–659
30. Gao C, Hao M, Chen J, Gu C (2021) Simulation and design of joint distribution of rainfall and tide level in Wuchengxiyu Region. China Urban climate 40:101005. https://doi.org/10.1016/j.uclim.2021.101005
31. Gascuel-Odoux C, Fovet O, Faucheux M, Salmon-Monviola J, Strohmenger L (2023) How to assess water quality change in temperate headwater catchments of western Europe under climate change: examples and perspectives Comptes Rendus. Géoscience. https://doi.org/10.5802/crgeos.147
32. Gidden MJ et al (2019) Global emissions pathways under different socioeconomic scenarios for use in CMIP6: a dataset of harmonized emissions trajectories through the end of the century. Geoscientific Model Devel 12(4):1443–1475. https://doi.org/10.5194/gmd-12-1443-2019
33. Gierszewski PJ, Habel M, Szmańda JB, Luc M (2019) Evaluating effects of dam operation on flow regimes and riverbed adaptation to those changes. Sci Total Environ 710:136202
34. Giuntoli I, Villarini G, Prudhomme C, Hannah DM (2018) Uncertainties in projected runoff over the conterminous United States. Clim Change 150(3–4):149–162
35. Gong S, Bai X, Luo G, Li C, Wu L, Chen, F.,... Zhang, S. (2023) Climate change has enhanced the positive contribution of rock weathering to the major ions in riverine transport. Global Planet Change 228:104203. https://doi.org/10.1016/j.gloplacha.2023.104203
36. Guan X, Zhang J, Elmahdi A, Li X, Liu J, Liu Y, Jin J, Liu Y, Bao Z, Liu C et al (2019) (2019) the capacity of the hydrological modeling for water resource assessment under the changing environment in semi-arid river Basins in China. Water 11:1328. https://doi.org/10.3390/w11071328
37. Guilpart E, Espanmanesh V, Tilmant A, Anctil F (2021) Combining split-sample testing and hidden Markov modelling to assess the robustness of hydrological models. Hydrol Earth Syst Sci 25:4611–4629. https://doi.org/10.5194/hess-25-4611-2021
38. Gupta HV, Sorooshian S, Yapo PO (1998) Toward improved calibration of hydrologic models: Multiple and noncommensurable measures of information. Water Resour Res 34:751–763
39. Hamby DM (1994) A review of techniques for parameter sensitivity analysis of environmental models. Environ Monit Assess 32:135–154. https://doi.org/10.1007/BF00547132
40. Hsu KC, Li ST (2010) Clustering spatial-temporal precipitation data using wavelet transform and self-organizing map neural network. Adv Water Resour 33:190–200
41. Huard D, Mailhot A (2008) Calibration of hydrological model GR2M using Bayesian uncertainty analysis. Water Resour Res 44:W02424
42. Huntington TG (2006) Evidence for intensification of the global water cycle: review and synthesis. J Hydrol 319:83–95
43. Ibrahim B, Wisser D, Barry B, Fowe T, Aduna A (2015) Hydrological Predictions for Small Ungauged Watersheds in the Sudanian Zone of the Volta Basin in West Africa. J Hydrol 4:386–397
44. Juneng L et al (2016) Sensitivity of Southeast Asia rainfall simulations to cumulus and air-sea flux parameterizations in RegCM4. Clim Res. https://doi.org/10.3354/cr01386
45. Kandekar VU, Pande CB, Rajesh J et al (2021) Surface water dynamics analysis based on sentinel imagery and Google Earth Engine Platform: a case study of Jayakwadi dam. Sustain Water Resour Manag 7:44. https://doi.org/10.1007/s40899-021-00527-7
46. Kay A, Griffin A, Rudd A, Chapman R, Bell V, Arnell N (2021) Climate change effects on indicators of high and low river flow across Great Britain. Adv Water Resour. 151:103909
47. Kendall M (1975) Multivariate Analysis. Charles Griffin & Company, London, p 202
48. Khoulé F (2020) Modélisation des impacts du changement climatique sur les ressources en eau du bassin versant du fleuve Casamance à Kolda. Physique et Applications, Université Assane Seck de Ziguinchor, Mémoire de Master, Mention, p 56
49. Kotlarski S, Keuler K, Christensen OB, Colette A, Déqué M, Gobiet A, Goergen K, Jacob D, Lüthi D, van Meijgaard E et al (2014) Regional climate modeling on European scales: A joint standard evaluation of the EURO CORDEX RCM ensemble. Geosci Model Dev 7:1297–1333
50. Kouassi AM, N'Guessan BTM, Kouame KF, Kouame KA, Okaingni JC, Biemi J (2012) Application de la méthode des simulations croisees a l'analyse de tendances dans la relation pluie-débit à partir du modèle GR2M : cas du bassin versant du N'zi-Bandama (Côte d'Ivoire). Comptes Rendus de l'Académie des Sciences, Géoscience, Tome 344:288–296
51. Kouassi A. M., 2007 : Caractérisation d'une modification éventuelle de la relation pluie-débit et ses impacts sur les ressources en eau en Afrique de l'Ouest : cas du bassin versant du N'zi (Bandama) en Côte d'Ivoire. Thèse de Docteur de l'Université de Cocody, Côte d'Ivoire, 234 p.
52. Li Y, Mi W, Ji L, He Q, Yang P, Xie, S.,... Bi, Y. (2023) Urbanization and agriculture intensification jointly enlarge the spatial inequality of river water

quality. Sci Total Environ 878:162559. https://doi.org/10.1016/j.scitotenv.2023.162559
53. Li J, Wang Z, Wu X, Xu C, Guo, S.,... Chen, X. (2020) Toward monitoring short-term droughts using a novel daily scale, standardized antecedent precipitation evapotranspiration index. J Hydrometeorol 21(5):891–908. https://doi.org/10.1175/JHM-D-19-0298.1
54. Liu Z, Xu J, Liu M, Yin Z, Liu X, Yin, L.,... Zheng, W. (2023) Remote sensing and geostatistics in urban water-resource monitoring: a review. Mar Freshw Res. https://doi.org/10.1071/MF22167
55. Luo J, Niu F, Lin Z, Liu M, Yin, G.,... Gao, Z. (2022) Abrupt increase in thermokarst lakes on the central Tibetan Plateau over the last 50 years. CATENA 217:106497. https://doi.org/10.1016/j.catena.2022.106497
56. M. Le Lay, 2006 : Modélisation hydrologique dans un contexte de variabilité hydroclimatique. Une approche comparative pour l'étude du cycle hydrologique à méso-échelle au Bénin. Thèse, Institut national polytechnique de Grenoble, France, 218.
57. Ma S, Qiu H, Yang D, Wang J, Zhu Y, Tang, B.,... Cao, M. (2023) Surface multi-hazard effect of underground coal mining. Landslides 20(1):39–52. https://doi.org/10.1007/s10346-022-01961-0
58. Mahfouz P, Mitri G, Jazi M, Karam F (2016) Investigating the Temporal Variability of the Standardized Precipitation Index in Lebanon. Climate 4:27. https://doi.org/10.3390/cli4020027Mann,H.B.NonparametricTestsagainstTrend,Econometrica.13(3),1945,245-259
59. Maraun D (2013) Bias correction, quantile mapping, and downscaling: Revisiting the inflation issue. J Climate 26:2137–2143
60. Markiewicz, M. Modelling of the air pollution dispersion, http://manhaz.cyf.gov.pl, Accessed 25 April 2010
61. Masood MU, Haider S, Rashid M, Aldlemy MS, Pande CB, Đurin B, Homod RZ, Alshehri F, Elkhrachy I (2023) Quantifying the impacts of climate and land cover changes on the hydrological regime of a complex dam catchment area. Sustainability 15(21):15223. https://doi.org/10.3390/su152115223
62. Mbaye ML, Sy K, Faty B, Sall SM (2020) Impact of 1.5 and 2.0 °C global warming on the hydrology of the Faleme river basin. J Hydrol 2020:100719. https://doi.org/10.1016/j.ejrh.2020.100719
63. Mbaye ML, Sylla MB, Tall M (2019) Impacts of 1.5 and 2.0 °C global warming on water balance components over Senegal in West Africa ? Atmos. 10(11):712. https://doi.org/10.3390/atmos10110712
64. Mendez M, Calvo-Valverde L-A, Imbach P, Maathuis B, Hein-Grigg D, Hidalgo-Madriz J-A, Alvarado-Gamboa L-F (2022) Hydrological response of tropical catchments to climate change as modeled by the GR2M Model: a case study in Costa Rica. Sustainability 14:16938. https://doi.org/10.3390/su142416938
65. Moradkhani, H.; Sorooshian, S. General Review of Rainfall–runoff Modeling: Model Calibration, Data Assimilation, and Uncertainty Analysis. In: Hsu, KL., Coppola, E., Tomassetti, B., Verdecchia, M., Visconti, G., (Eds); *Hydrological Modelling and the Water Cycle*; Water Science and Technology Library; Sorooshian, Springer: Berlin/Heidelberg, Germany, 2018.
66. Mouelhi S, Michel C, Perrin C, Andreassian V (2006) Linking stream flow to rainfall at the annual time step: the Manabe bucket model revisited. J Hydrol. https://doi.org/10.1016/j.jhydrol.2005.12.022
67. Mouelhi S, Michel C, Perrin C, Andréassian V (2006) Stepwise development of a two parameter monthly water balance model. J Hydrol 318:200–214
68. Mouelhi S., 2003 : *Vers une chaîne cohérente de modèles pluie-débit conceptuels globaux aux pas de temps pluriannuel, annuel, mensuel et journalier*. Thèse de Doctorat, ENGREF, Cemagref Antony, France, 323 p.
69. Mubialiwo A, Abebe A, Onyutha C (2021) Performance of rainfall – runoff models in reproducing hydrological extremes: a case of the River Malaba sub-catchment. SN Appl Sci 3:24. https://doi.org/10.1007/s42452-021-04514-7
70. Nie S, Mo S, Gao T, Yan B, Shen P, Kashif, M.,... Jiang, C. (2023) Coupling effects of nitrate reduction and sulfur oxidation in a subtropical marine mangrove ecosystem with Spartina alterniflora invasion. Sci Total Environ 862:160930. https://doi.org/10.1016/j.scitotenv.2022.160930
71. Nief H, Paturel JE, Servat E (2003) Study of parameter stability of a lumped hydrologic model in a context of climatic variability. J Hydrol 278:213–230
72. N'guessan K, Kouassi AM, Gnaboa R, Traoré KS, Houenou PV (2014) Analyse de phénomènes hydrologiques dans un bassin versant urbanisé: cas de la ville de Yamoussoukro (Centre de la Cote d'Ivoire). Larhyss J 17:135–154
73. OMVG, 2012 : Plan d'Action GIRE du bassin versant du fleuve Kayanga/Géba Volume 3 : Portfolio de projets, Facilité Africaine de l'Eau, 125 p.
74. Ojeda W; Martínez P; Hernández L. 2008. Repercussions of Climate Change on Irrigated Agriculture. In: Martínez P, Aguilar A (Eds); Effects of Climate Change on Mexico's Water Resources Mexican Institute of Water Technology. Morelos; Mexico
75. Okkan U, Fistikoglu O (2014) Evaluating climate change effects on runoff by statistical downscaling and hydrological model GR2M. Theor Appl Clim 117:343–361
76. Olsson J, Arheimer B, Borris M, Donnelly C, Foster K, Nikulin G, Persson M, Perttu A-M, Uvo C, Viklander M et al (2016) Hydrological climate change impact assessment at small and large scales: key messages from recent progress in Sweden. Climate 4:39
77. O'Neill BC, Tebaldi C, van Vuuren D, Eyring V, Friedlingstein P, Hurtt G et al (2016) The scenario model intercomparison project (ScenarioMIP) for CMIP6. Geosci Model Devel 9:3461–3482. https://doi.org/10.5194/gmd-9-3461-2016
78. Pande CB (2020) Sustainable watershed development planning. In: Sustainable watershed development. SpringerBriefs in water science and technology. Springer, Cham. https://doi.org/10.1007/978-3-030-47244-3_4
79. Pande CB, Al-Ansari N, Kushwaha NL, Srivastava A, Noor R, Kumar M, Moharir KN, Elbeltagi A (2022) Forecasting of SPI and meteorological drought based on the artificial neural network and M5P model tree. Land 11(11):2040. https://doi.org/10.3390/land11112040
80. Pande CB, Moharir KN, Singh SK et al (2022) Groundwater flow modeling in the basaltic hard rock area of Maharashtra, India. Appl Water Sci 12:12. https://doi.org/10.1007/s13201-021-01525-y
81. Parajka J, Merz R, Blöschl G (2007) Uncertainty and multiple objective calibration in regional water balance modelling: case Study in 320 Austrian Catchments. Hydrol Processes 21:435–446
82. Perrin C., 2000 : *Vers une amélioration d'un modèle global pluie-débit au travers d'une approche comparative.* Thèse de Doctorat, Institut National Polytechnique de Grenoble, France, 287 p
83. Piani C, Haerter JO, Coppala E (2010) Statistical bias correction for daily precipitation in regional climate models over Europe. Theor Appl Climatol 99:187–192
84. Projet d'Appui au Développement Rural en Casamance (PADERCA) 2008 : Etablissement de la situation de référence du milieu naturel en basse et moyenne Casamance. République du Sénégal Ministère de l'Agriculture Rapport final, 201 p
85. Pérez-Sánchez J, Senent-Aparicio J, Segura-Méndez F, Pulido-Velazquez D, Srinivasan R (2019) Evaluating hydrological models for deriving water resources in Peninsular Spain. Sustainability 11:2872
86. Qiu D, Zhu G, Bhat MA, Wang L, Liu Y, Sang, L.,... Sun, N. (2023) Water use strategy of nitraria tangutorum shrubs in ecological water delivery area of the lower inland river: based on stable isotope data. J Hydrol 624:129918. https://doi.org/10.1016/j.jhydrol.2023.129918
87. Qiu D, Zhu G, Lin X, Jiao Y, Lu S, Liu, J.,... Chen, L. (2023) Dissipation and movement of soil water in artificial forest in arid oasis areas: cognition based on stable isotopes. CATENA 228:107178. https://doi.org/10.1016/j.catena.2023.107178
88. Quesada-Chacón D, Barfus K, Bernhofer C (2021) Climate change projections and extremes for Costa rica using tailored predictors from CORDEX model output through statistical downscaling with artificial neural networks. Int J Climatol 41:211–232
89. Rameshwaran P, Bell VA, Davies HN et al (2021) How might climate change affect river flows across West Africa? Clim Change. https://doi.org/10.1007/s10584-021-03256-0
90. Rau P, Bourrel L, Labat D, Ruelland D, Frappart F, Lavado W, Dewitte B, Felipe O (2019) Assessing Multidecadal Runoff (1970–2010) using regional hydrological modelling under data and water scarcity conditions in peruvian pacific catchments. Hydrol Proc 33:20–35
91. Rivas-Acosta, I. Effects of Climate Change on Mexico's Water Resources (Surface Water); Mexican Institute of Water Technology: Morelos, Mexico, 2015; ISBN 978–607–9368–09–8
92. Rui S, Zhou Z, Jostad HP, Wang L, Guo Z (2023) Numerical prediction of potential 3-dimensional seabed trench profiles considering complex

motions of mooring line. Appl Ocean Res 139:103704. https://doi.org/10.1016/j.apor.2023.103704
93. Réméniéras (1976) La variabilité climatique et son impact sur les ressources en eau dans le degré carré de Grand-Lahou (Sud-Ouest de la 'ôte d'Ivoire). Articles. https://doi.org/10.4000/physio-geo.1581
94. Sagna P (2005) Dynamique du climat et de son évolution récente dans la partie ouest de l'Afrique occidentale. Université Cheikh Anta Diop de Dakar, Thèse de Doctorat d'Etat, p 786
95. Saha GC, Quinn M (2020) Integrated surface water and groundwater analysis under the effects of climate change, hydraulic fracturing and its associated activities: a case study from Northwestern Alberta. Canada Hydrology 7:70
96. Sané T, Sy O, Dieye EHB (2011) Changement climatique et vulnérabilité de la ville de Ziguinchor. Actes du colloque "Renforcer la résilience au changement climatique des villes : du diagnostic spatialisé aux mesures d'adaptation" (2R2CV) 07 et 08 juillet 2011, Université Paul Verlaine - Metz, France, 1–14
97. Seibert J, Vis MJP (2012) Teaching hydrological modeling with a user-friendly catchment-runoff-model software package. Hydrol Earth Syst Sci 16:3315–3325
98. Shen M, Chen J, Zhuan M, Chen H, Xu C-Y, Xiong L (2018) Estimating uncertainty and its temporal variation related to global climate models in quantifying climate change impacts on hydrology. J Hydrol 556:10–24
99. Singh SK, Marcy N (2017) Comparison of simple and complex hydrological models for predicting catchment discharge under climate change. AIMS Geosci 3(3):467–497
100. Sood A, Smakhtin V (2015) Global hydrological models: a review. Hydrol Sci J 60:549–565
101. Soro G, Yao A, Kouame Y, Bi T (2017) Climate change and its impacts on water resources in the Bandama Basin. Côte D'ivoire Hydrol 4:18
102. Teutschbein C, Seibert J (2012) Bias correction of regional climate model simulations for hydrological climate-change impact studies: review and evaluation of different methods. J Hydrol 456:12–29
103. The Climate Atlas of Canada, Version 2 (July 10, 2019), using data from BCCAQv2 climate models, The Climate Atlas of Canada, Version 2, 2019,
104. Thompson JR, Iravani H, Clilverd HM, Sayer CD, Heppell CM, Axmacher JC (2017) Simulation of the hydrological impacts of climate change on a restored floodplain. Hydrol Earth Syst Sci 62:2482–2510
105. Tian H, Huang N, Niu Z, Qin Y, Pei, J. Wang, J. (2019) Mapping winter crops in China with Multi-source satellite imagery and phenology-based algorithm. Remote Sensing 11(7):820. https://doi.org/10.3390/rs11070820
106. Tian H, Pei J, Huang J, Li X, Wang J, Zhou, B.,... Wang, L. (2020) Garlic and winter wheat identification based on active and passive satellite imagery and the google earth engine in Northern China. Remote sensing 12(3539):3539. https://doi.org/10.3390/rs12213539
107. Topalović Ž, Todorović A, Plavšić J (2020) Evaluating the transferability of monthly water balance models under changing climate conditions. Hydrol Sci J 65:928–950
108. de Vos NJ, Rientjes THM (2005) Constraints of artificial neural networks for rainfall–runoff modelling: Trade-offs in hydrological state representation and model evaluation. Hydrol Earth Syst Sci 9:111–126
109. Wu X, Guo S, Qian S, Wang Z, Lai C, Li, J.,... Liu, P. (2022) Long-range precipitation forecast based on multipole and preceding fluctuations of sea surface temperature. Int J Climatol 42(15):8024–8039. https://doi.org/10.1002/joc.7690
110. Wu B, Quan Q, Yang S, Dong Y (2023) A social-ecological coupling model for evaluating the human-water relationship in basins within the Budyko framework. J Hydrol 619:129361. https://doi.org/10.1016/j.jhydrol.2023.129361
111. Xi X, Xi B, Miao C, Yu R, Xie J, Xiang, R.,... Hu, F. (2022) Factors influencing technological innovation efficiency in the Chinese video game industry: applying the meta-frontier approach. Technol Forecast Soc Chang 178:121574. https://doi.org/10.1016/j.techfore.2022.121574
112. Xu C, Xu Y (2012) (2012) The projection of temperature and precipitation over China under RCP scenarios using a CMIP5 multi-model ensemble. Atmos Ocean Sci Lett 5(6):527–533
113. Xue Y, Bai X, Zhao C, Tan Q, Li Y, Luo, G.,... Long, M. (2023) Spring photosynthetic phenology of Chinese vegetation in response to climate change and its impact on net primary productivity. Agric For Meteorol 342:109734. https://doi.org/10.1016/j.agrformet.2023.109734
114. Yang Y, Liu L, Zhang P, Wu F, Wang Y, Xu, C.,... Kuzyakov, Y. (2023) Large-scale ecosystem carbon stocks and their driving factors across Loess Plateau. Carbon Neutr 2(1):5. https://doi.org/10.1007/s43979-023-00044-w
115. Yin Z, Liu Z, Liu X, Zheng W, Yin L (2023) Urban heat islands and their effects on thermal comfort in the US: New York and New Jersey. Ecol Ind 154:110765. https://doi.org/10.1016/j.ecolind.2023.110765
116. Yin L, Wang L, Ge L, Tian J, Yin Z, Liu, M.,... Zheng, W. (2023) Study on the thermospheric density distribution pattern during geomagnetic activity. Appl Sci. https://doi.org/10.3390/app13095564
117. Yin L, Wang L, Li T, Lu S, Yin Z, Liu, X.,... Zheng, W. (2023) U-Net-STN: a novel end-to-end lake boundary prediction model. Land 12(8):1602. https://doi.org/10.3390/land12081602
118. Zhou G, Deng R, Zhou X, Long S, Li W, Lin G, Li X (2021) Gaussian inflection point selection for LiDAR hidden echo signal decomposition. IEEE Geosci Remote Sens Lett. https://doi.org/10.1109/LGRS.2021.3107438
119. Zhou G, Li W, Zhou X, Tan Y, Lin G, Li X, Deng R (2021) An innovative echo detection system with STM32 gated and PMT adjustable gain for airborne LiDAR. Int J Remote Sens 42(24):9187–9211. https://doi.org/10.1080/01431161.2021.1975844
120. Zhou G, Zhang R, Huang S (2021) Generalized buffering algorithm. IEEE access 9:27140–27157. https://doi.org/10.1109/ACCESS.2021.3057719
121. Zhu X, Xu Z, Liu Z, Liu M, Yin Z, Yin, L.,... Zheng, W. (2022) Impact of dam construction on precipitation: a regional perspective. Mar Freshw Res. https://doi.org/10.1071/MF22135
122. Zubler EM, Fischer AM, Fröb F, Liniger MA (2016) Climate Change Signals of CMIP5 General Circulation Models over the Alps-Impact of Model Selection. Int J Climatol 36:3088–3104

Publisher's Note